Machine Design (MCG 3131 A)

Lateral Offset Gear Reducer

...The Infamous but Superb Mickey Mouse Drawbridge

Created and Designed By:

Sharon Tam - 8172069

Dan Bornstein - 8482732

Osman El-Ghotmi - 8091726

Michael Botros - 8327615

For: Dr. Ahsan Faraz Ahmed

Machine Design Project

Date: Tuesday, July 24th, 2018

University of Ottawa

I. Abstract

This report will outline the combined efforts of Sharon Tam, Dan Bornstein, Osman El-Ghotmi, and Michael Botros in the design of a gearbox system with the following specifications: it operates on a power of 5 Hp and converts an input rotation speed of 100 rpm to an output rotation speed of 15 rpm with use of an lateral offset arrangement of the input and output shafts. The report will also highlight the early stages of brainstorming, decision making, mechanical analysis, mechanical design, and feasibility of the system. Ultimately, a gearbox with a horizontal arrangement of shafts (input and output shafts are laterally offset), spur gears, radial contact ball bearings and a sand cast casing with two-halves that are bolted, was designed to satisfy the specifications. The high torque generated by this gearbox would be useful in turning the bridge deck of the drawbridge at Disney World's well-known castle.

II. Table of Contents

III. List of Figures

IV. List of Tables

1.0 Introduction

The purpose of this project is for the following mechanical engineering students: Sharon Tam, Dan Bornstein, Osman El-Ghotmi, and Michael Botros to have the opportunity to work in collaboration and design a stand-alone gear reducer. The design constraint is to create a lateral offset gear configuration with an input power of 5 HP, input angular speed of 100 rpm, and an output angular speed of 15 rpm. These specifications, in turn, will require an overall speed ratio of 6.667 or in other words, an output angular speed that is 0.15 times the input angular speed for the lateral offset gear reducer.

The application and reason for this design is to provide a reliable, efficient, and cost-effective gear reduction solution for a commercial drawbridge. The design constraints for the gear reducer are a perfect match for the requirements needed by the drawbridge.

In deciding the most suitable configuration for this design, five critical factors will be taken into account. These factors are reliability, maintenance, sizing, cost, and noise. Furthermore, an in depth analysis of the gear configuration, the catalog gears, and the bearing types will be done to ensure the system is mechanically feasible.

The design procedure will be concluded with a computer aided design in order to provide a visual illustration of the concept for the approval of technical authorities.

2.0 Theoretical Background

The general purpose of a gear reducer is to convert a high input angular speed to a low output angular speed. This low speed provides two advantages, one of which is a higher output torque in heavy rotational load scenarios, and improved system stability (reduced vibrations).

A low output angular speed, a high output torque and stability are required in lowering and raising the bridge deck of a drawbridge castle, where the deck is heavy, and thus requires a slow and forceful rotation for lowering and raising the bridge. In this application, heavy rotation loads are induced on the pivot of the drawbridge.

Traditionally, the power (approximately 5 Hp) by standard electric motors do not provide the sufficient torque to rotate the door pivot of a drawbridge, thus a gear reducer must be integrated at the interface between source (the electric motor connected to the gear reducer input shaft) and the remaining output mechanisms of the drawbridge.

The input and output shafts of a gear reducer can be placed in several different orientations. Typically, the shafts are designed to be parallel or perpendicular to each other, though there are instances in which the shafts are offset by an angle to the other. The shaft axes also can either intersect each other or not intersect at all. The gear reducer shaft orientation discussed in this report will be the lateral offset orientation. Lateral offset implies that the input and output shafts are parallel to each other, but they are not collinear.

The system is a simple shaft mounted reducer that receives a belt driven input, where the output shaft is directly coupled to the drawbridge shaft [4].

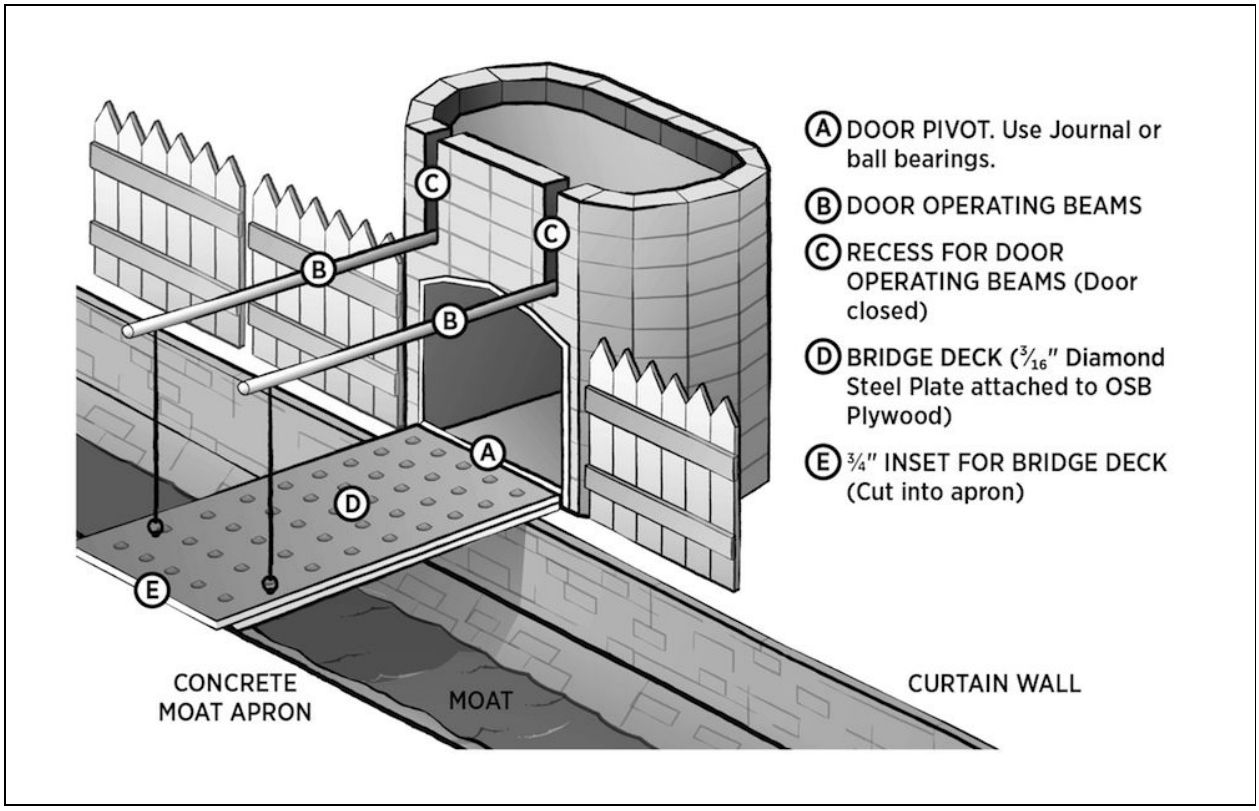

Figure 1. Concept Drawing of a Disney Castle Drawbridge

This is a technical drawing of a Disney Drawbridge. The figure points to the various mechanical components of the drawbridge and it is important to pay attention to item C and item B on the diagram. These two mechanical parts are a door recess and operating beam. The Infamous but Superb Mickey Mouse Drawbridge will have an input shaft that is belt driven at a constant rate of 100 rpm. The output shaft will then drive the door recess at a constant rate of 15 rpm.

3.0 Generation of Solutions

Members of the design team proposed three different gearbox solutions to consider in the decision matrix when deciding upon one solution to carry out in its design. Each solution shows the configuration of the shafts, the types of gears chosen and the types of bearings chosen.

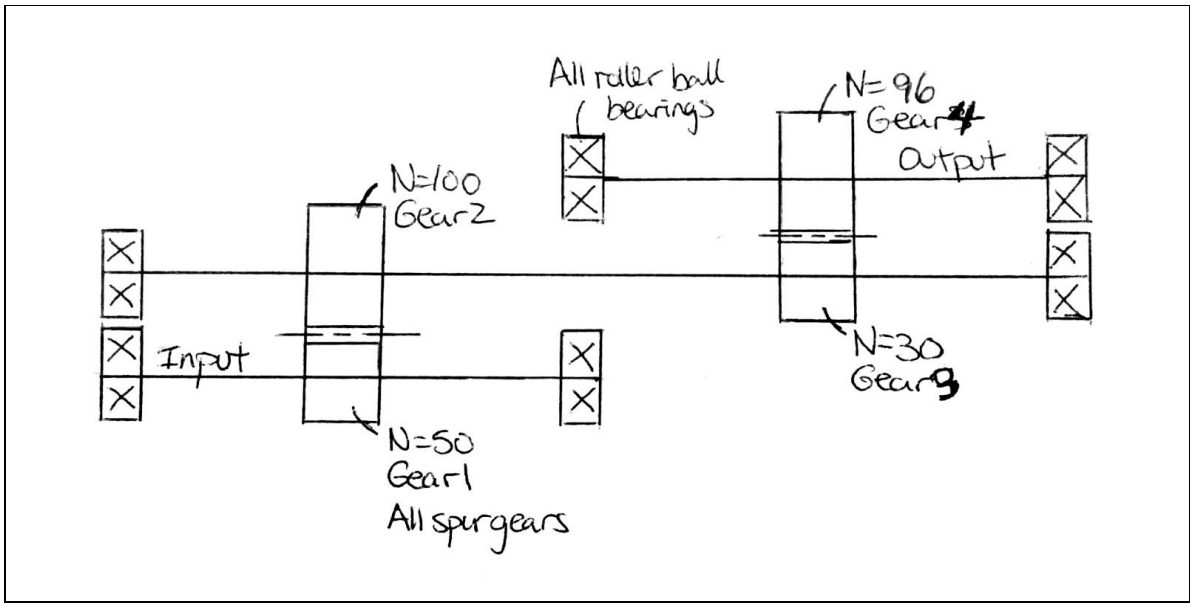

Figure 2. Solution 1 - Distinguished by Spur Gears and Parallel Shafts

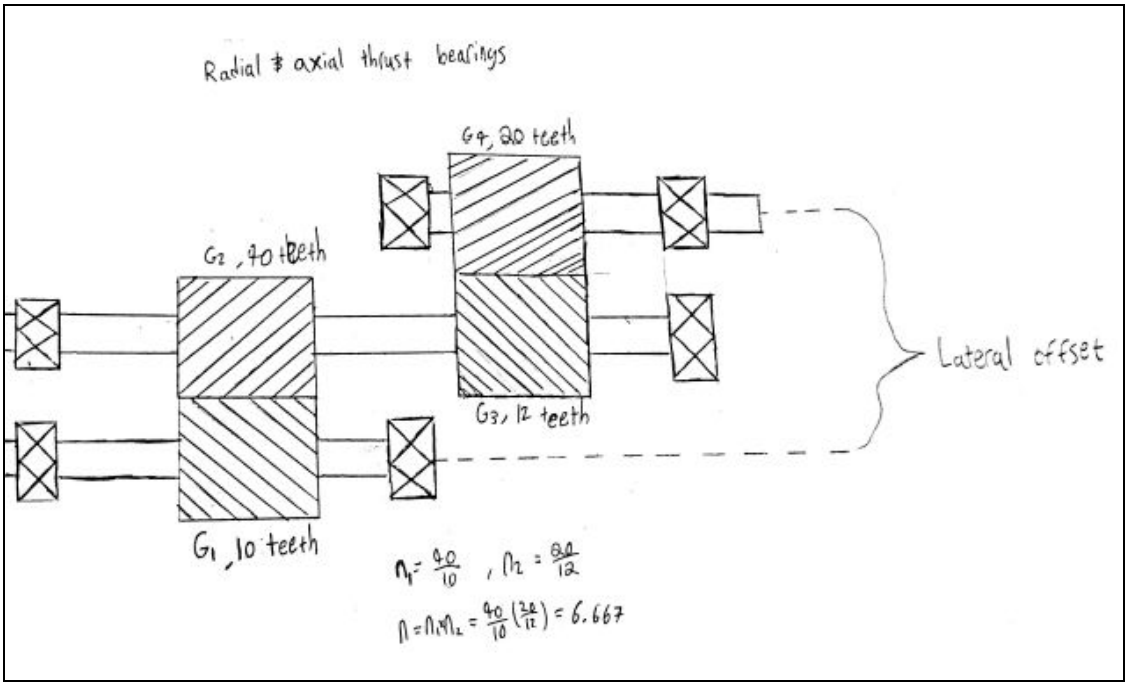

Figure 3. Solution 2 - Distinguished by Helical Gears and Parallel Shafts

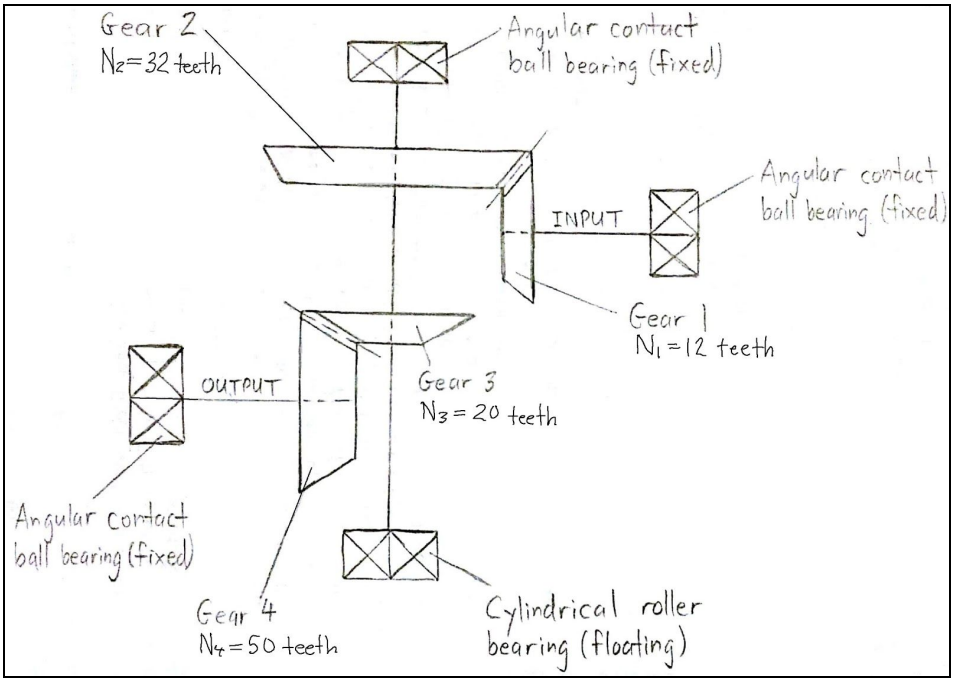

Figure 4. Solution 3 - Distinguished by Bevel Gears and Perpendicular Shafts

Table 1 summarizes the characteristics of these three possible combinations of gears and bearings for two different shaft configurations.

Table 1. Possible Solutions to Designing the Gear Reducer

Gear Reducer Component	**Shaft Configurations**		
	Configuration 1 (Parallel Shafts)		Configuration 2 (Perpendicular Shafts)
	Solution 1	Solution 2	Solution 3
Gear Types	Spur	Helical	Bevel
Bearing Types	Radial ball bearings on each shaft	Axial and thrust bearings on each shaft	Angular contact ball bearings fixed on all shafts and cylindrical roller bearing floating on the continuous shaft

3.1 Design Choice Based on the Decision Matrix

From solutions 1, 2, and 3, the solution choice for the speed reducer design was determined using a decision matrix with the following 5 weighted criteria:

1) **Reliability**: This criterion refers to the overall mechanical reliability of the speed reducer and how effective it will be at withstanding the operational stresses and fatigue loading over time. Gear and bearing configurations should aim to minimize contact stresses as well the axial and radial loads on the shafts themselves.

Reliability was given the highest weight since the goal is to have a functioning speed reducer, and any mechanical failure would render the design useless.

2) **Maintenance**: A design's maintenance score is dependant on the simplicity of the design and how easy it is to provide regular maintenance (i.e. repairs) to the speed reducer. Some factors include part availability, the mounting processes as well as the shaft configurations.

Maintenance was given the second highest weight due to the importance of long term use which effective and simple maintenance facilitates.

3) **Sizing**: This criterion refers to how compact the overall design can be made. Some limited factors are the gear sizing, and how many gears and bearings on a given shaft.

Sizing was given the second lowest weight since a drawbridge motor doesn't rely on compact design as it isn't a high precision instrument. The only sizing decisions made were for the stability of the system, but a drawbridge doesn't prioritize the highest stability.

4) **Cost**: This refers to the overall price to order the gears, bearings, and shafts as well as the assembly of the speed reducer. Components with higher availability and less intensive manufacturing process are prioritized due to their lower associated cost.

Cost was given a moderate importance with a weight of 3 since low cost is essential to amusement parks that would purchase the drawbridge opener, but it was decided that the cost shouldn't compromise the overall effectiveness of the mechanical design.

5) **Noise**: This factor refers to how much noise is produced by the speed reducer. This is largely dependant on the gear selections.

Noise was given the lowest priority due to the noise not being factored into the mechanical performance, and the drawbridge being used outdoors where noise is not a factor. It still isn't considered a negligible factor due to Disney World being a family friendly environment.

Solution 1: Parallel shafts and Spur Gears

The spur gear system was given the highest score for maintenance due to the ease of removing spur gears directly from the shafts as well as the fact that standard spur gears are the most readily available and replaceable components. This system also had the best score for the cost since spur gears are the cheapest and most readily available.

Solution 1 had the second highest ranking for reliability since spur gear systems tend to have slightly higher contact stresses than helical gears but similar loading on the shafts. The sizing scores was determined to be second since out of the three solutions, solution 1 had the second smallest diameter gears.

Lastly solution 1 had the lowest ranking for noise since there is an increase in noise associated with the lower contact area.

Solution 2: Parallel Shafts and Helical Gears

For solution 2, the reliability and sizing scores score were the highest due to the smoothness of operation for helical gears and also the helical gears chosen were the smallest set of gears out of the three. Solution 2 also had the highest score for noise since the smoothness of helical gears/ high contact area allows for the lowest noise.

The mounting process for helical gears and the radial/thrust bearings required is not as easy as the mounting process for spur gears which leaves helical gears with a lower score for maintenance. Helical gears also had a lower score for cost since they are more expensive due to not being straight cut like spur gears.

Solution 3: Perpendicular Shafts and Bevel Gears

Solution 3 had the lowest overall scores in the decision matrix for maintenance due to the lower availability of the gears as well as the challenges in maintaining a system with two 90° shifts in the shafts. It also had the lowest score for sizing due to having the largest diameter gears.

Overall solution 3 is not recommended since bevel gears aren't necessary since the 90° shift between shafts is not necessary in a speed reducer that is laterally offset.

Table 2 shows the individual criterion scores and the total scores for each solution based on how well it satisfies the criteria previously defined.

Table 2. Decision Matrix - Assessment of How Each Solution Satisfies Each Criteria on a Scale of 0 (Very Poor) to 5 (Very Good)

Criteria:		**Reliability**	**Maintenance**	**Sizing**	**Cost**	**Noise**	**Weighted Totals**
Weights:		**5**	**4**	**2**	**3**	**1**	
Solution 1 Scores	Unweighted	4	5	4	5	2	65
	Weighted	20	20	8	15	2	
Solution 2 Scores	Unweighted	5	3	5	3	4	60
	Weighted	25	12	10	9	4	
Solution 3 Scores	Unweighted	3	3	3	4	3	48
	Weighted	15	12	6	12	3	

Solution 1 is the most appropriate choice for the speed reducer. The high reliability, ease of maintenance, and low cost of a spur gear system were all essential factors in choosing this design over solutions 2 and 3.

4.0 Design Analysis Approach and Assumptions

This section outlines the procedure used to design the gearbox and the assumptions made when referring to "Machine Component Design" by R. Juvinall and K. Marshek (J&M textbook) [5] to find the required values for the design equations.

The approach for designing a speed reducer began with the gear selection. Once gears were chosen, it was necessary to run calculations to confirm the viability of the gears. Before any stress-based safety factors were determined, it was necessary to confirm that every gear pairing did not have any interference. This task was done by calculating the contact ratios and checking if they were above a minimum value of 1.2 [5].

Initially small gears made of 1020 As Rolled Steel were chosen, but this had to be adjusted due to the generally low input and output speeds given by the design restrictions. The low speeds and high torques led to much higher tangential forces than expected. In order to ensure acceptable safety factors for the gears in surface fatigue and bending stresses, larger sized gears were chosen from the Boston Gear Catalogue. This made the material availability limited to higher strength steels and cast iron.

Many assumptions had to taken during the gear selection process in order to make the gear selection process feasible without physical testing. It was assumed that the gears have a 99% reliability, have a life of 10 million cycles, and that the loads are being applied at the tip of each tooth in contact (no load sharing). Since it is not necessary for this particular speed reducer do be a high precision instrument, we assumed less rigid mountings, less accurate gears, and contact across the full face of the gears in order to determine the mounting correction factors (K_m). Based on a suggestion from the Boston Gear Catalogue, it was assumed that the gears would be produced using a hobs form cutter and the corresponding velocity factor (K_v) was selected. Lastly, for the application of a drawbridge, it was assumed that the source of power would be uniform with a moderate level of shock for the machinery and an appropriate overload correction factor (K_o) was chosen.

Once the gear selection process was completed, it was possible to determine the reaction forces at the bearing positions as well as the loading diagrams across each shaft. Since the gears chosen were significantly larger than expected, it was no longer a reasonable assumption to treat the weights of the gears and shafts as negligible. Instead, an assumption was made that the gear weights could be point loads at the centre of each gear and the shaft weights could be point loads centered between two bearings. On the other hand, shear force was neglected due to its impact on shear stress being negligible in comparison to torsion. Since spur gears were used for this design, axial forces were negligible. Not only did neglecting axial forces allow us to use radial bearings only, it made it a reasonable assumption that the components did not need to be press fitted onto the shafts, and that retaining rings were sufficient for the mounting process.

The length of the shafts were chosen to be reasonably short in order to limit the deflection and likelihood of bending failure. In addition, the gears were positioned in a symmetrical fashion to ensure even distribution of loads across each bearing. Once the gear positioning was known, equilibrium calculations were done, and shear, bending moment and torque diagrams were produced for each shaft with the assistance of the SkyCiv Cloud Engineering software.

Additionally, the shafts diameters varied across each shaft according the bore diameters of the gears and bearings. Any location with a change in diameter produced a stress concentration. In order to determine the bending safety factor and the torsion safety factor for each shaft, a set of critical points (i.e. points on shaft where failure is most likely) were chosen for safety factor calculations. Any point with a stress concentration factor (e.g. a shaft step or a keyway) or any point with maximum loading was chosen as a critical point. The points with stress concentration factors were intentionally placed in locations with minimal loading. For the shafting analysis, the loading was assumed to be alternate reversed bending with a constant torque. Due to the low rotation speeds of the shafts, the heat produced by friction was assumed to be negligible, and due to the gearbox being used indoors, it was assumed that the temperature would not affect the mechanical durability of the system.

Once the mean and alternating stresses, and the relevant stress concentration factors were determined using the loading values from the diagrams and the relevant textbook graphs and tables respectively, the endurance limits were calculated for each form of loading on each shaft. Then, the safety factors were calculated using the Modified Goodman Criterion. A satisfactory safety factor (n) was in this range: $1 < n \leq 3$. In the case of any safety factor being less than satisfactory, the shaft material would be replaced by a material with a higher ultimate strength (S_u).

SkyCiv also provided some deflection values which were essential to determine if our shafts rotated below the critical speed limit. Angle of twist calculations were also carried out to determine if the shafts were within the tolerance of shaft twist per shaft length affected by torque (the tolerance is 1^o/ft).

Next, calculations were done to design the necessary key lengths to transmit the necessary torque from one gear to another. Before these calculations were done, it was first necessary to ensure that the capacity torque for a given key was higher the the torque values in the load diagrams. It was assumed that the shaft keyways were made using the Sled Runner method; this assumption was necessary to determine keyway stress concentration factors (K_f). As for the key widths and heights, they are the gear keyway widths and heights provided by the Boston Gears Catalogue.

Subsequently, the necessary clearance values for each bearing were determined using catalogue information. Then, shaft diameters and shaft step locations near the bearings were chosen. It was assumed that journal bearing were not necessary since the friction and temperatures were low enough for roller bearings with oil based lubrication to be sufficient.

Finally, a casing was designed such that each shaft has a fixed-floating bearing arrangement and such that the gearbox would be easy to assemble practically.

4.1 Selection of Specific Gears and Bearing Types

Since an important design criteria was maintenance which includes part availability in the market, options for gears were taken from the Boston Gear catalog with the title “Gears, Couplings and Shaft Accessories”, and options for the types of bearings to be used were taken from the “NTN Ball and Roller Bearings” catalog. These catalogs are trusted and parts coming from them are readily available in the market [2 and 3].

Before selecting catalog gears, one must take into account the diametral pitch of a gear as well as the required overall angular speed reduction of the gear.Eq. 1 gives an expression for the diametral pitch P, where N is the number of gear teeth and d is the gear pitch diameter [1].

$$P = \frac{N}{d} \qquad \text{(Eq. 1)}$$

For any two gears to be able to mesh, they must have the same diametral pitch, that is to say, their teeth need to equally spaced out along the circumference. From the catalog, for each reduction stage, gears with the same diametral pitch of 5 were selected for the first reduction, and gears with a diametral pitch of 3 were selected for the second reduction.

The speed ratio R of one stage of speed reduction is given by Eq. 2 where n_p is the rotational speed of the pinion, n_g is the rotational speed of the gear, N_p is the number of teeth on the pinion (the driving gear) and N_g is the number of teeth on the gear (the driven gear) [1].

$$R = \frac{n_p}{n_g} = \frac{N_g}{N_p} \qquad \text{(Eq. 2)}$$

Gears were chosen from the catalog such that the speed reduction stages are even (i.e. all speed reduction stages have approximately the same speed reduction). Even reduction stages allow for all pinions to be approximately the same size and all gears to be approximately the same size; this sizing technique allows the gearbox to be as compact as possible. In addition, even reduction stages allow for an even distribution of bending moments among the shafts because if some gears are quite larger in diameter than other gears, then the bending moments on the shaft(s) with the larger gears would be quite higher than those with smaller gears.

Considering that gears on the same shaft have the same rotational speed and applying Eq. 2 for each speed reduction stage in the gear train (for each pair of meshing gears) yields Eq. 3, where n_i is the input rotational speed of the gear reducer, n_o is its output rotational speed, $\frac{n_i}{n_o}$ is its overall angular speed ratio, $\Pi N_{driving}$ is the product of the teeth of all driving gears and ΠN_{driven} is the product of the teeth of all driven gears [1].

$$\frac{n_i}{n_o} = \frac{\Pi N_{driven}}{\Pi N_{driving}} \qquad \text{(Eq. 3)}$$

For this gear reducer, the speed ratios chosen for each stage in speed reduction were 2 and 3.2 (ideally 2 and 3.33) for gears 1 and 2, and gears 3 and 4 respectively. The overall speed ratio is 6.4, so gears were chosen from the catalog to satisfy this speed ratio closely.

In order to determine which gears were appropriate for the aforementioned speed ratios, the minimum pinion teeth and the maximum gear teeth for each speed reduction stage needed to be calculated. This can be done by applying Eq.4 and 5 below for the minimum pinion teeth as well as Eq. 2. N_p is the minimum number of teeth on the pinion, N_g is the maximum number of teeth on the gear, ϕ is the pressure angle, R is the speed ratio, k is a constant equal to 1 for full-depth teeth and 0.8 for stub teeth. The constant is taken as 1 in the calculations [1].

$$N_p = \frac{2k}{(1+2R)sin^2\phi}\left(R + \sqrt{R^2 + (1+2R)sin^2\phi}\right) \quad \text{(Eq. 4)}$$

$$N_g = \frac{N_p^2 sin^2\phi - 4k^2}{4k - 2N_p sin^2\phi} \quad \text{(Eq. 5)}$$

The minimum number of teeth for gear 1, with a pressure angle of 20°, was calculated to be 15, so a gear with 50 teeth was chosen . For gear 2, the maximum number of teeth possible is infinity since the pinion has more than 18 teeth and a pressure angle of 20°, so the gear chosen has 100 teeth to a gear ratio of 2, . [7] For gear 3, the minimum number of teeth, for a pressure angle of 14.5°, was calculated to be 29, so a gear with 30 teeth was chosen. For gear 4, the maximum number of teeth is calculated to be 220, so to be close to the ideal ratio 3.33, the number of teeth need to be around 100 so a gear with 96 teeth was chosen for a ratio of 3.2. Sample calculations are shown in Appendix C-1. The gears chosen are summarized in Table 3.

Table 3. Gears Chosen from Boston Gears Catalogue [3]

Gear	Catalog Number	Number of Teeth	Pressure Angle (°)	Pitch Diameter (in.)	Bore Diameter (in.)	Face Width (in.)	Overall Length (in.)	Keyway or Set Screw
1	YK50	50	20	10.00	1.250	2.500	3.750	Both
2	YK100	100	20	20.00	1.500	2.500	4.250	Both
3	NO30B	30	14.5	10.00	1.4375	3.000	4.250	Both
4	NO96B	96	14.5	32.00	1.9375	3.000	4.750	Both

Based on the type of gears selected (spur, helical, bevel, etc.), and the magnitudes and types of loads they undergo (radial, axial and thrust loads), bearing types were chosen from the catalog and analyzed in Section 4.3.

4.2 Design Analysis of the Gears

This portion of the report will provide a brief explanation for the procedure involved in determining effectiveness and feasibility of the gears selected for this design. Some of the important formulas are as follows in Eq. 6, 7, 8, 9, 10, and 11. Eq. 6 is the linear speed (V) equation, where d_p is the pitch diameter of the pinion, and n is the angular velocity of the pinion.

$$V = \frac{\pi d_p n}{12} \quad \text{(Eq. 6)}$$

Eq. 7 is the tangential force calculation, where H is the power in horsepower.

$$F_t = \frac{33000H}{V} \quad \text{(Eq. 7)}$$

Eq. 8 and 9 calculate the diametral and base pitches. p is the diametral pitch, P is the pitch, p_b is the base pitch, and ϕ is the pressure angle. Eq. 10 calculates the base radius r from the pitch radius r_b, or half of the pitch diameter.

$$p = \frac{\pi}{P} \quad \text{(Eq. 8)}$$

$$p_b = p\cos(\phi) \quad \text{(Eq. 9)}$$

$$r_b = r\cos(\phi) \quad \text{(Eq. 10)}$$

Eq. 11 calculates the contact ratio CR. In this equation, r_p is the pitch radius of the pinion, r_g is the pitch radius of the gear, and the other variables are defined as in the above equations. [5]

$$CR = \frac{\sqrt{(r_p+P^{-1})^2 - r_p^2\cos^2\phi} + \sqrt{(r_g+P^{-1})^2 - r_g^2\cos^2\phi} - (r_p+r_g)\sin\phi}{p_b} \quad \text{(Eq. 11)}$$

It is important to first determine if the contact ratio between the pinion and the gear is acceptable. The above formula helps to determine the contact ratio and any contact ratio that is greater than 1.2 is acceptable for the design. This formula requires that we calculate the base pitch which is done by using catalogue information for the diametral pitch and pressure angle. The rest of the information is provided in the catalogue and is used to calculate the contact ratio as per the above formula.

Once the contact ratio is confirmed to be acceptable, analysis of the gears may begin. There are two types of fatigue calculations that need to be done, as the gear is constantly under stress when running.

One of the fatigue calculations that need to be executed is bending fatigue. The goal of the calculations is to determine if the safety factor for gears under cyclic bending loads is acceptable, meaning it is above 1. Eq. 12 is for bending fatigue strength S_n. The endurance limit S'_n is determined to be half the ultimate strength S_u as seen in Eq. 13. C_L is the load factor,

C_G is the gradient factor, C_S is the surface factor, k_r is the reliability factor, k_t is the temperature factor, and k_{ms} is the mean stress factor.

$$S_n = S'_n C_L C_G C_s k_r k_t k_{ms} \quad \text{(Eq. 12)}$$

$$S'_n = 0.5 S_u \quad \text{(Eq. 13)}$$

Each of the above listed factors are evaluated using tables and figures from the Juvinall and Marshek textbook. After evaluating these factors and determining the ultimate strength of the material in question, the endurance limit of the gear can be calculated using the equation provided in Eq. 12. This can apply to both the pinion and gear. The two equations below, Eq. 14 and 15, are used then to find the stress of the gear σ and then the safety factor n of said gear. Most of the variables are defined as above. Those who are not yet defined are the velocity factor K_v, the overload factor K_o, the mounting correction factor K_m, and the geometry factor J. These factors can be obtained in the textbook, except for the geometry factor for the gears with a pressure angle of 14.5°. That factor was obtained from the AGMA-908-B39 information sheet [6]. These factors were determined separately for each gear [5].

$$\sigma = \frac{F_t P}{bJ} K_v K_o K_m \quad \text{(Eq. 14)}$$

$$n = \frac{S_n}{\sigma} \quad \text{(Eq. 15)}$$

The other fatigue calculations that need to be done are the surface fatigue stress calculations. These calculations are used to determine if the safety factor for gears that experience constant surface loading is acceptably above 1. From the textbook, the constants for velocity factor K_v, overload factor K_o, mounting correction factor K_m, life factor C_{Li}, reliability factor C_R, surface fatigue strength S_{fe}, and elastic coefficient C_p were obtained to

be used in the following equation. Eq. 16 permits for the calculation of the gears actual surface fatigue strength S_H, and Eq. 17 calculates the corresponding surface stresses σ_H that will actually be acting on it. I is a separate geometry factor for surface fatigue. It can be calculated using Eq. 18 below using the pressure angle ϕ and gear ratio R. The Eq. 19 allows us to determine the safety factor.

$$S_H = S_{fe} C_{Lip} C_R \quad \text{(Eq. 16)}$$

$$\sigma_H = C_p \cdot \sqrt{\frac{F_t}{b d_p I} K_v K_o K_m} \quad \text{(Eq. 17)}$$

$$I = \frac{\sin\phi \cos\phi}{2} \frac{R}{R+1} \quad \text{(Eq. 18)}$$

$$n = \frac{S_H}{\sigma_H} \quad \text{(Eq. 19)}$$

Complete sample calculations are shown in Appendix C-2. The results of the calculations are tabulated in Table 4. [5]

Table 4. Results of the Design Analysis of the Gears

	Gear 1	**Gear 2**	**Gear 3**	**Gear 4**
Bending Stress Fatigue				
Bending Stress σ (psi)	13033.23	11771.95	11462.99	10316.69
Ultimate Strength S_u (psi)	31000	31000	31000	31000
Endurance Limit S'_n (psi)	15500	15500	15500	15500
Bending Fatigue Strength S_n (psi)	15014.23	15014.23	15014.23	15014.23
Safety Factor n	**1.15**	**1.28**	**1.31**	**1.46**
Surface Stress Fatigue				
Elastic Coefficient C_p ($psi^{1/2}$)	1800	1800	1800	1800
Surface Stress σ_H (psi)	46982.31	46982.31	56073.98	56073.98
Surface Fatigue Strength S_{fe} (psi)	70000	70000	70000	70000
Gear Tooth Surface Fatigue Strength S_H (psi)	70000	73500	73500	77000
Safety Factor n	**1.49**	**1.56**	**1.31**	**1.37**

4.3 Design Analysis of the Shafts

The first thing to determine in the design analysis of the shafts is to evaluate the tangential and radial forces produced by each of the gears in the system. The requirements of the system is to sustain an input power of 5 hp at 100 rpm (at the driving end of the input shaft) and an output of 15 rpm (at the driven end of the output shaft). Given the diameters, teeth numbers, pressure angles, and configuration of the gear systems, the tangential and radial forces can be computed with the following general formulas for spur gear calculations.

$$Gear\ Velocity = V = \frac{\pi dn}{12} = Feet\ per\ Minute$$

$$Tangential\ Force = F_t = \frac{33000H}{V} = Pounds\ of\ Force$$

$$Radial\ Force = F_r = F_t * tan\phi = Pounds\ of\ Force$$

Where:

$V = Velocity\ (fpm)$

$d = Diameter\ (in)$ $n = Revolution\ Rate\ (rpm)$

$F_t = Tangential\ Force\ (lbf)$

$H = Power\ (horsepower)$

$F_r = Radial\ Force\ (lbf)$

$\phi = Pressure\ Angle\ (deg)$

Given the magnitudes of each of these values calculating the forces acting on each gear becomes rather simple. Furthermore, these values allow for the calculation of the reaction forces that will be acting on the bearings that are to be placed on either end of each shaft. Another thing to consider is the effective weight of the gears and the shafts. On smaller scale systems,

these forces would usually be considered negligible and thus neglected. However, the gears and shafts required for our system are much larger and neglecting these forces could become problematic if safety factors are not high enough. For this reason, all forces that result from gravity will also be taken into consideration for this analysis. It is also important to note that shafts 1 and 3 slightly extend out of the gearbox to allow space for the input and output of torque. This would slightly shift the center of mass of the shafts. Since this shift is very small and the weight of the shafts have a small effect when compared to the other forces acting on the system, the center of mass will be assumed to be at the center distance between the two bearings. Within the scope of the project, this procedure will produce reliable results.

$$Input\ Torque = F_{t1}(d_1/2) = (630.25)(10/2) = 3151.25\ lb \bullet in$$

Weight of Gears :

$W_{G1} = 57.66\ lbf$

$W_{G2} = 216.88\ lbf$

$W_{G3} = 74.37\ lbf$

$W_{G4} = 656.82\ lbf$

Weight of Shafts :

$W_{S1} = 20.87\ lbf$

$W_{S2} = 43.07\ lbf$

$W_{S3} = 50.13\ lbf$

The following pages will outline the reaction forces at each of the bearings and their respective radial loads. This will be done by evaluating any forces acting on the shafts as a result of the gears or gravitational forces. Each of the shafts will have their sum of moments and force evaluated in both the x-y and x-z planes. All forces in the x direction (axial forces) are assumed

to be zero. Figure 5 shows a simplified schematic of the shafts and mounting features considered in the equilibrium calculations; shafts AB, CD and EF are the input, intermediate and output shafts respectively.

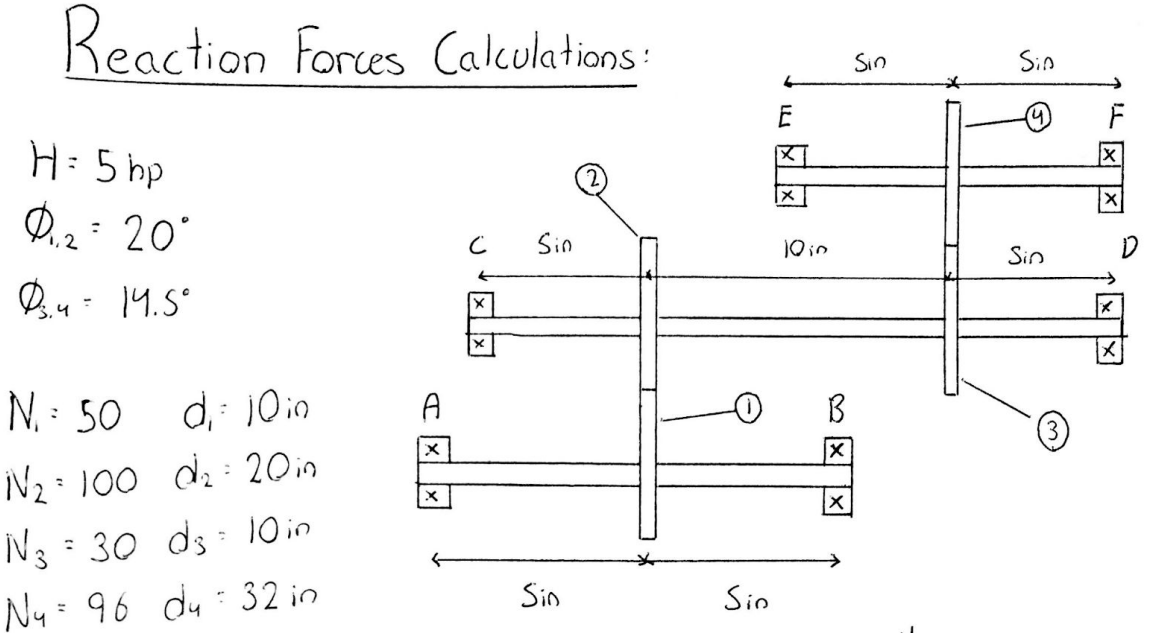

Figure 5. Simplified Schematic of Shafts and Mounting Features Considered in Equilibrium

For shaft AB, a hand-drawn free-body diagram (FBD) and a SkyCiv-generated FBD are displayed in Figures 6 and 7 respectively. The corresponding FBDs for shaft CD are shown in Figures 8 and 9 and those for shaft EF are shown in Figures 10 and 11. Calculations for the reaction forces in each shaft can be seen in Appendix C-3.

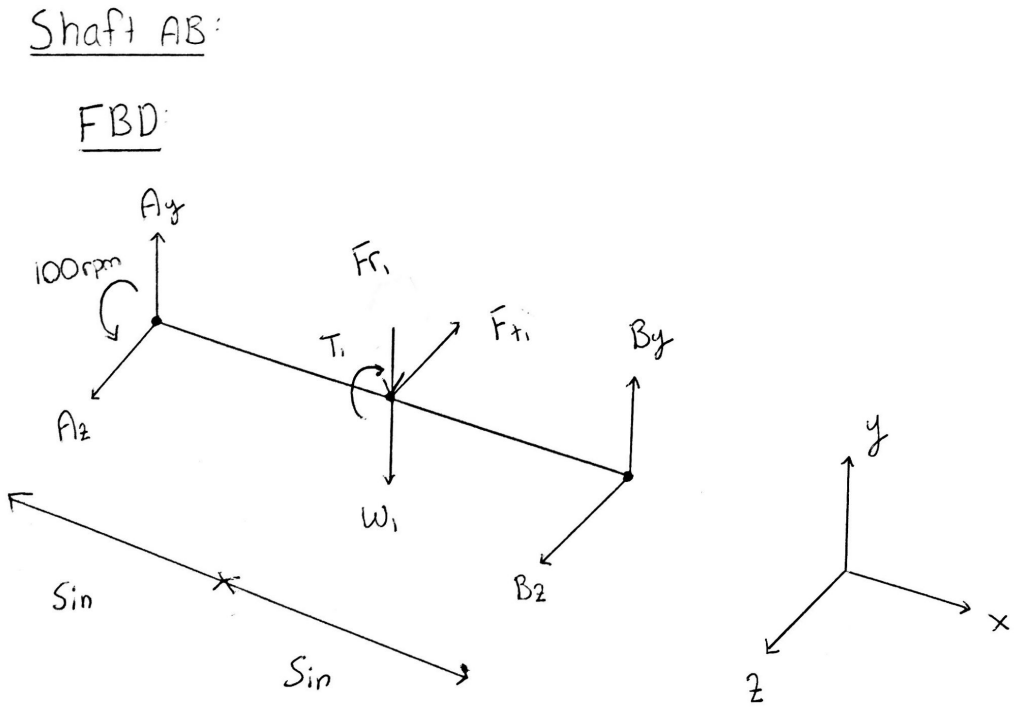

Figure 6. Hand-drawn FBD of Shaft AB

Figure 7. SkyCiv-generated FBD of Shaft AB (All Dimensions in Inches and Bearing Centerlines Identified in Green)

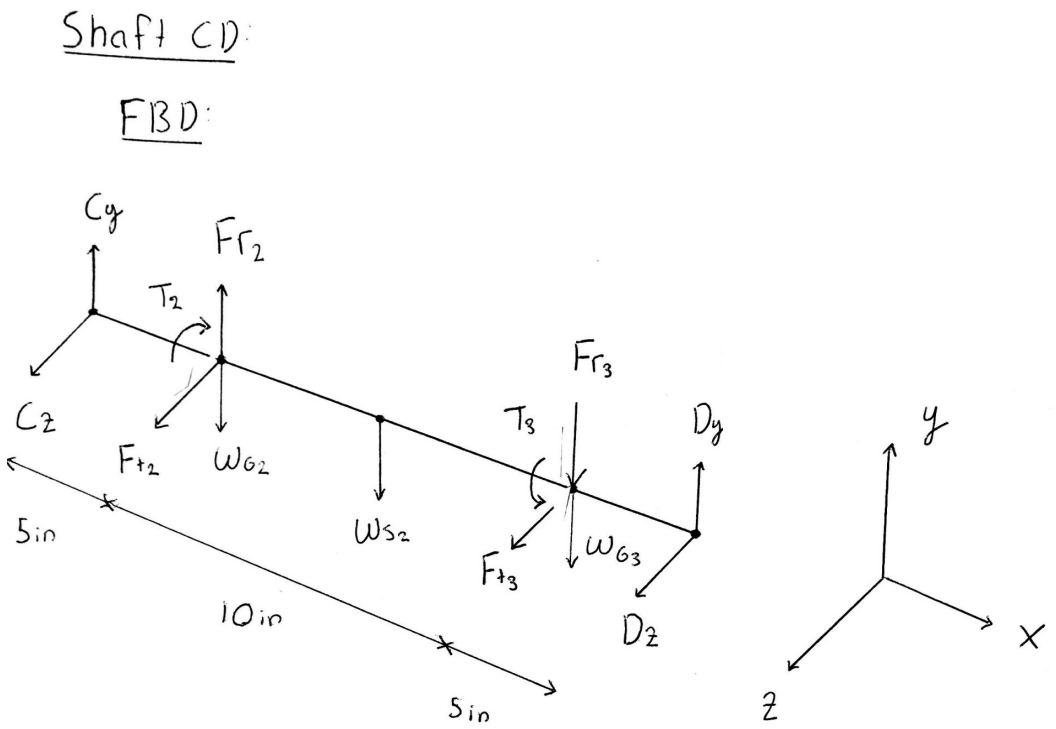

Figure 8. Hand-drawn FBD of Shaft CD

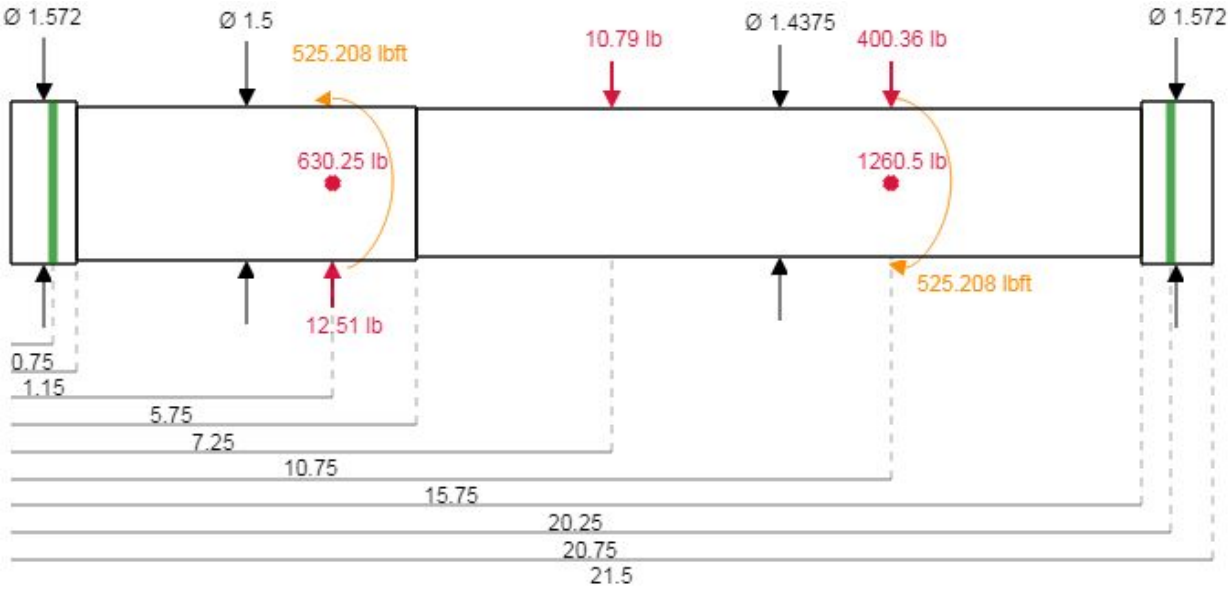

Figure 9. SkyCiv-generated FBD of Shaft CD (All Dimensions in Inches and Bearing Centerlines Identified in Green)

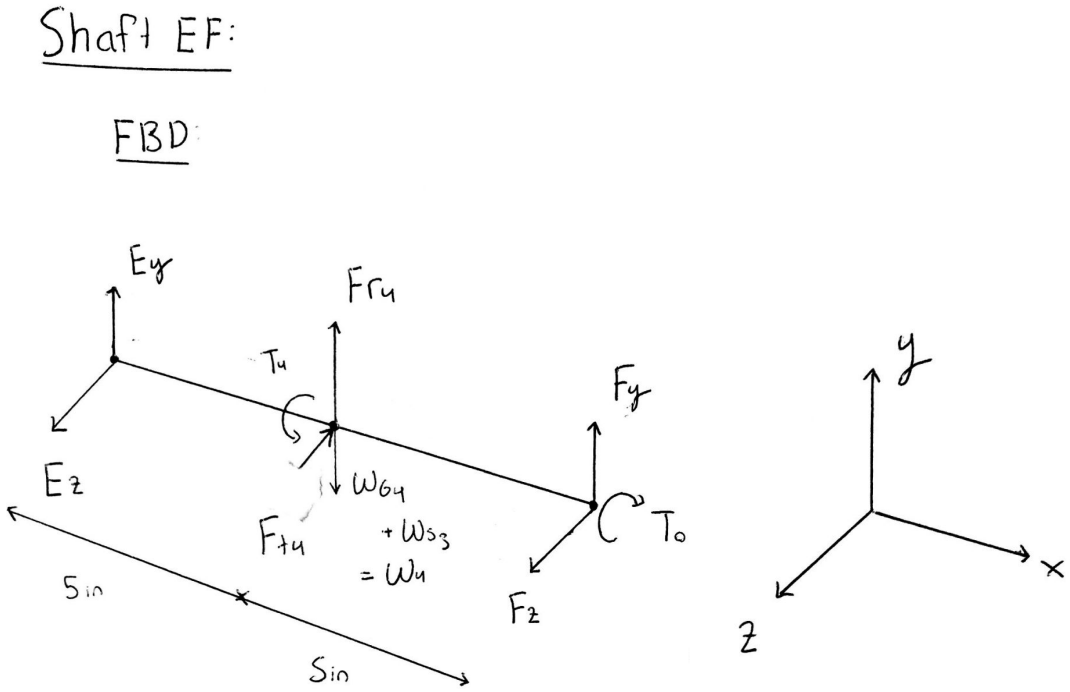

Figure 10. Hand-drawn FBD of Shaft EF

Figure 11. SkyCiv-generated FBD of Shaft EF (All Dimensions in Inches and Bearing Centerlines Identified in Green)

The next step in the design of the gearbox was to create diagrams for the shear force, bending moment and torque along the shafts.

Eq. 20 shows the relationship used to determine the shear force at different distances (x) along the shaft ($\frac{dV(x)}{dx}$ is the rate of change of shear force with respect to distance along the shaft and w(x) is the distributed load as a function of x):

$$\frac{dV(x)}{dx} = w(x) \qquad \text{(Eq. 20)}$$

According to this equation, point loads indicate where the shear force steps up or down in the diagram.

Eq. 21 shows the relationship used to determine the bending moment at different distances (x) along the shaft ($\frac{dM(x)}{dx}$ is the rate of change of bending moment with respect to distance along the shaft and V(x) is the shear force as a function of x):

$$\frac{dM(x)}{dx} = V(x) \qquad \text{(Eq. 21)}$$

With this equation, the slope of line segments in the bending moment diagram at a location x is the value of the shear force at this same location. This concept is demonstrated in Appendix B where the shear force diagrams and bending moment diagrams are shown for all the shafts in both the x-y and x-z planes. All load diagrams were drawn with the SkyCiv Cloud Engineering software which was verified to produce results that matched the results coming from Eq. 20 and 21. [5]

Furthermore, for each shaft, diagrams were created for the vector sum of the shear forces and bending moments. For each line segment of those diagrams, Pythagorean theorem was applied as shown in Eq. 22 and 23. V is the vector sum of the shear force in the xy plane (V_y) and the shear force in the xz plane (V_z) and M is the vector sum of the bending moment in the xy plane (M_z, moment acting in the z direction) and the bending moment in the xz plane (M_y, moment acting in the y direction).

$$V = \sqrt{V_y^2 + V_z^2} \qquad \text{(Eq. 22)}$$

$$M = \sqrt{M_y^2 + M_z^2} \qquad \text{(Eq. 23)}$$

Diagrams for the vector sum of the shear forces and bending moments are respectively shown in Figures 12 and 13 for the input shaft, Figures 14 and 15 for the intermediate shaft and Figures 16 and 17 for the output shaft. [5]

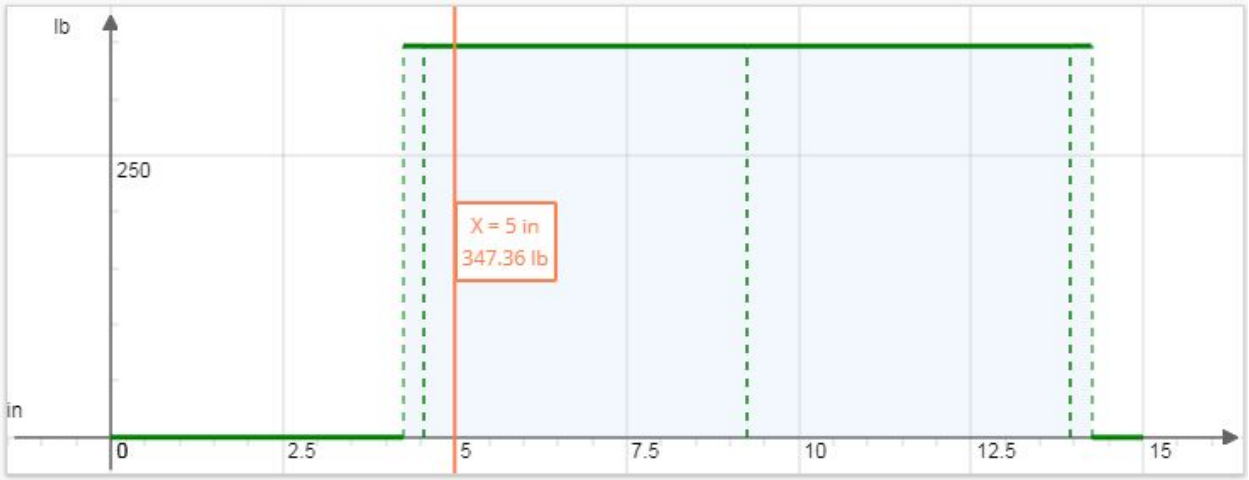

Figure 12. Vector Sum of the Shear Force as a Function of Distance x along the Input Shaft

Figure 13. Vector Sum of the Bending Moment as a Function of Distance x along the Input Shaft

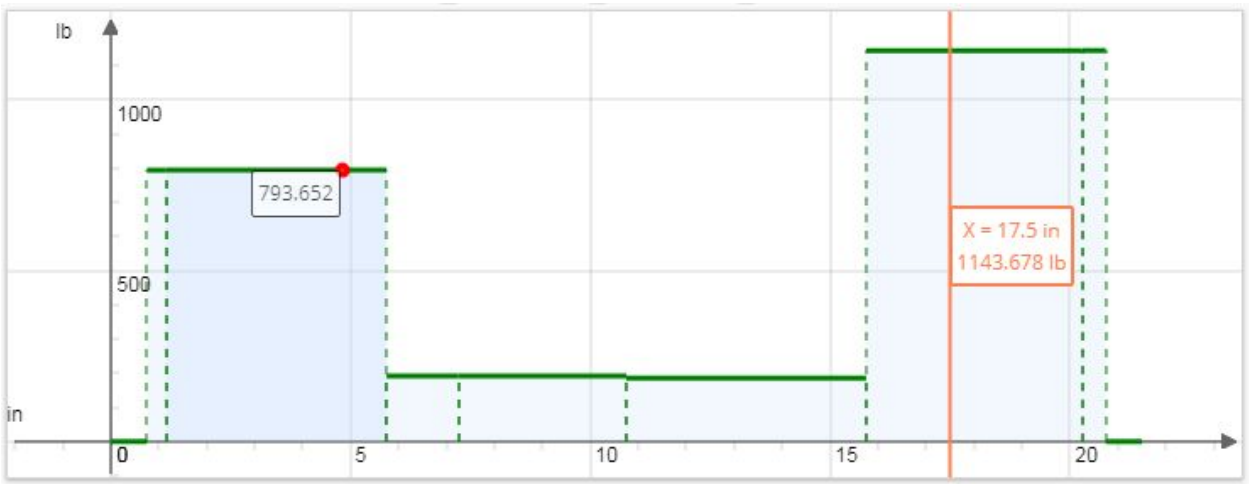

Figure 14. Vector Sum of the Shear Force as a Function of Distance x along the Intermediate Shaft

Figure 15. Vector Sum of the Bending Moment as a Function of Distance x along the Intermediate Shaft

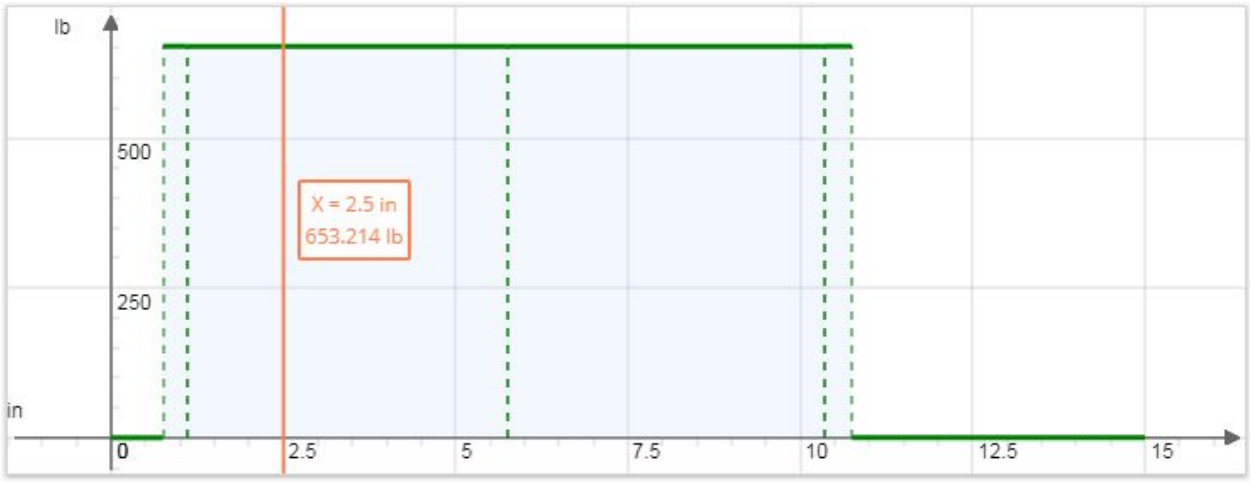

Figure 16. Vector Sum of the Shear Force as a Function of Distance x along the Output Shaft

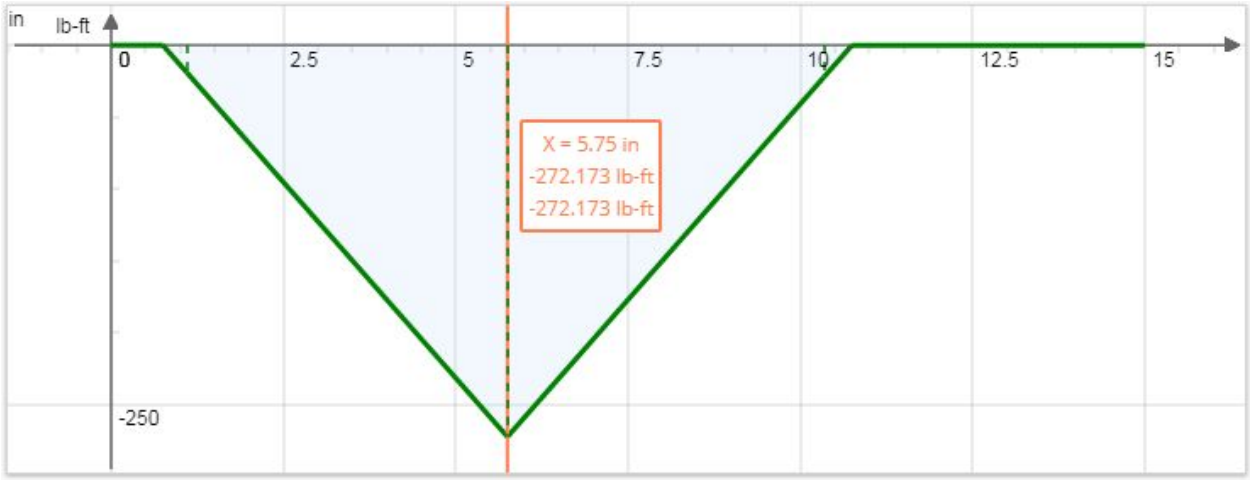

Figure 17. Vector Sum of the Bending Moment as a Function of Distance x along the Output Shaft

Torque diagrams were then created by considering for each shaft, the lengths between applied and reaction torques. The torque was treated as constant starting from the applied torque and ending at the reaction torque further down the shaft. Figures 18, 19 and 20 represent the torque diagrams for the input, intermediate and output shafts respectively.

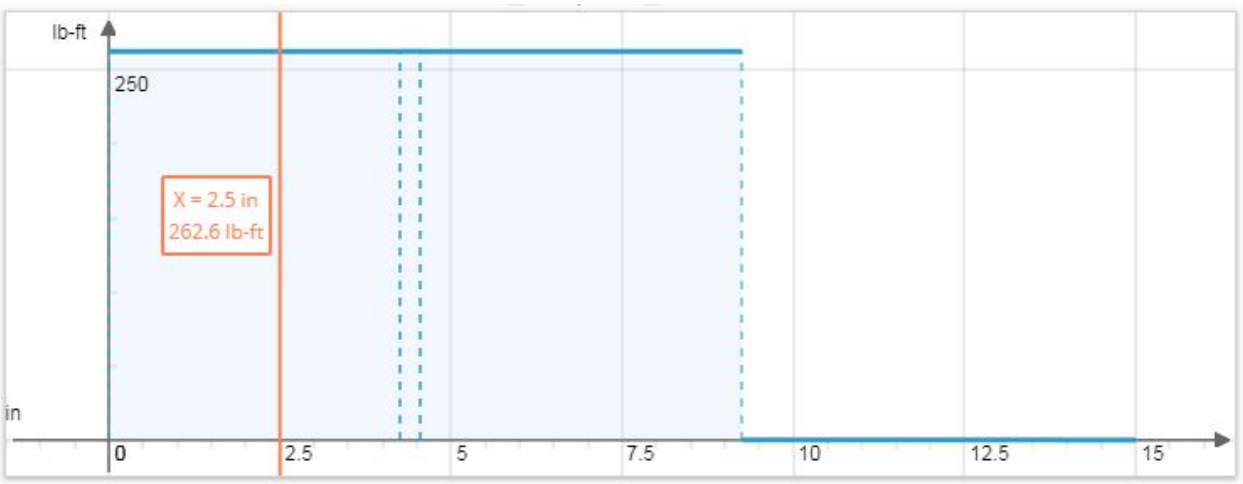

Figure 18. Torque as a Function of Distance x along the Input Shaft

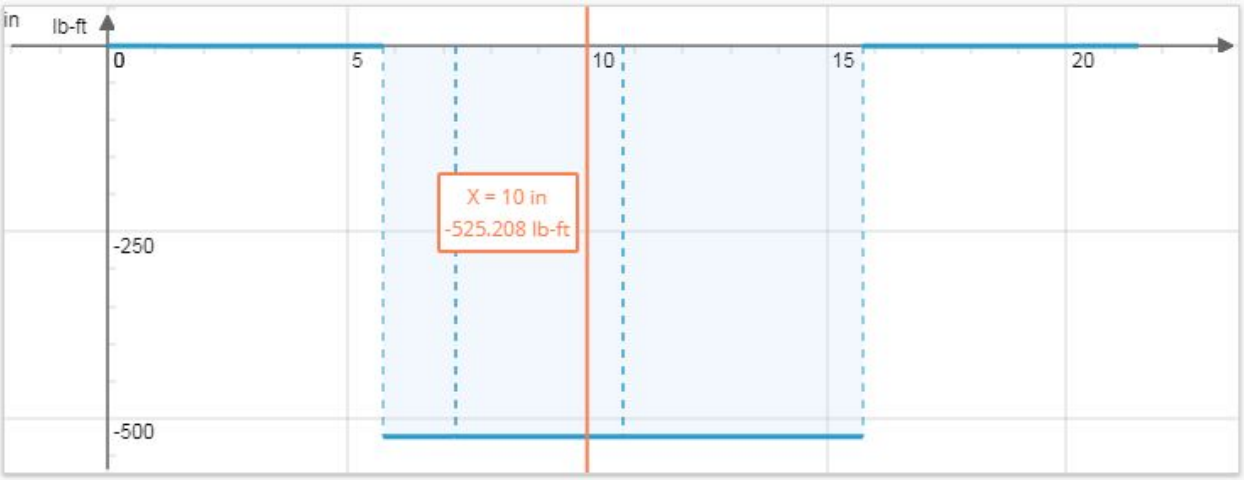

Figure 19. Torque as a Function of Distance x along the Intermediate Shaft

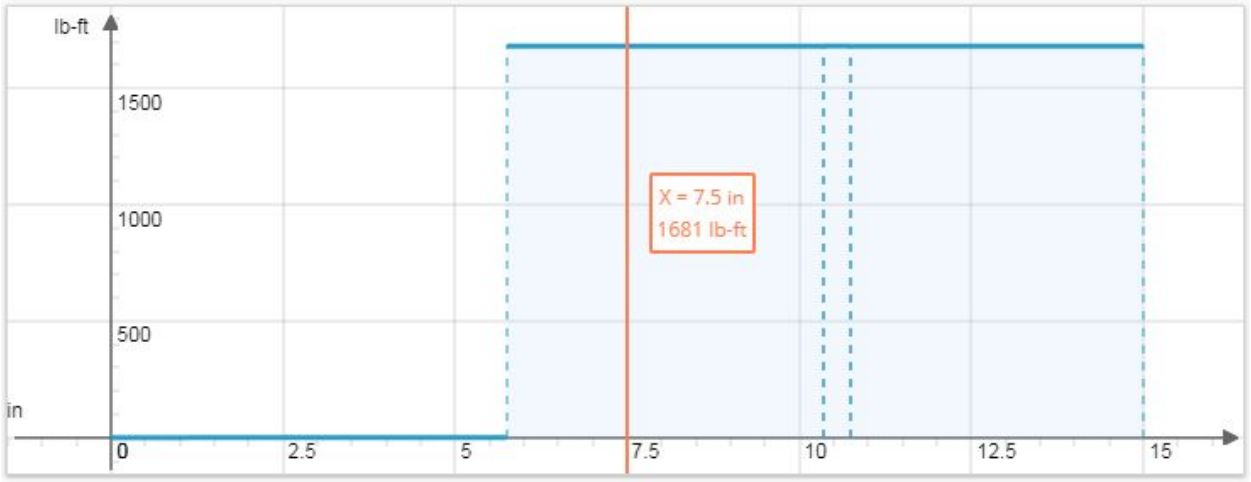

Figure 20. Torque as a Function of Distance x along the Output Shaft

After the load diagrams were created, an analysis of the safety factors of the shaft was done. The safety factors were for the two main causes of stress in the shaft, namely bending and torsion. These factors were calculated using the Modified Goodman Criterion, seen below in Eq. 24, at critical points. σ_{ea} is the effective alternating stress, calculated in Eq. 25 with concentration factor K_f, the alternating moment M_a, the shear concentration factor K_{fs}, and the alternating torque T_a. σ_{em} is the effective mean strength, calculated in Eq. 26 using the same concentration factors, the mean moment M_m, and the mean torque T_m.

$$\frac{\sigma_{ea}}{S_n} + \frac{\sigma_{em}}{S_u} = \frac{1}{n} \quad \text{(Eq. 25)}$$

$$\sigma_{ea} = \frac{16}{\pi d^3}\sqrt{4K_f M_a{}^2 + 3K_{fs} T_a{}^2} \quad \text{(Eq. 26)}$$

$$\sigma_{em} = \frac{16}{\pi d^3}(K_f M_m + \sqrt{K_f M_m{}^2 + K_{fs} T_m{}^2}) \quad \text{(Eq. 27)}$$

The critical points were determined to be at the location of any sudden diameter changes (also known as steps), any groove such as a keyway, and the point where the shaft experiences the highest bending and torsion forces. These points can cause a concentration of stresses such that a material can fail at a lower stress, or fail locally but not anywhere else along the shaft.

Other critical calculations for the shaft include the torsional deflection θ, and critical speed n_{crit} calculations. The torsional deflection can be used to determine the rate of twist, which cannot be more than 1°/foot of shaft. The critical speed is the speed at which vibrations start to become problematic in a shaft. It is recommended that the operating speed is at least half the critical speed. Eq. 28 calculates the torsional deflection according to the torque T, the diameter of the shaft d, and the shear modulus G. The shear modulus values were obtained from the Juvinall and Marshek textbook, as well as Matweb [5 and 8]. Eq. 29 and 30 calculate the critical speed for single and multiple mass configurations respectively. δ_{st} and δ are the static deflections, g is the gravitational constant, and w is the force applied. [5]

$$\theta = \Sigma \frac{32TL}{\pi G d^4} \quad \text{(Eq. 28)}$$

$$n_{crit} = \frac{30}{\pi}\sqrt{\frac{g}{\delta_{st}}} \quad \text{(Eq. 29)}$$

$$n_{crit} = \frac{30}{\pi}\sqrt{\frac{g\Sigma w\delta}{\Sigma w\delta^2}} \quad \text{(Eq. 30)}$$

A full sample calculation is provided in Appendix C-4 for a step in shaft CD.

The keyway dimensions are also an integral part of the shaft calculations to determine how long of a keyway slot must be cut. The width and height of the key are already dictated by the keyway cut into the gears chosen, so the only calculations needed are to determine the length of key needed such that the key will not shear in proper usage of the gearbox. Eq 31, 32 and 33 are used to do so, where T is torque, S_y is the yield strength of the shaft, L is the length of the key and d is the diameter of the shaft to which is key is mounted. [5]

$$T = \frac{\pi d^3}{16}(0.58S_y) \quad \text{(Eq. 31)}$$

$$T = S_y \frac{Ld}{8}\frac{d}{2} = S_y \frac{Ld^2}{16} \quad \text{(Eq. 32)}$$

$$T = 0.58S_y \frac{Ld^2}{8} \quad \text{(Eq. 33)}$$

The results of the calculations are summarized below in Tables 5, 6, 7, 8 and 9. Shaft CD has the lowest safety factor, and as such, is more prone to failure.

Table 5. Results of the Design Analysis of Critical Points on Shaft AB

	Keyway for Gear 1	**Step by Bearing A**	**Step by Bearing B**
Ultimate Strength S_u (psi)	129300	129300	129300
Endurance Limit S'_n (psi)	64650	64650	64650
Bending Fatigue Strength S_n (psi)	36469.19	36469.19	36469.19
Torsion Fatigue Strength S_n (psi)	21152.13	21152.13	21152.13
Mean Stress σ_{em} (psi)	11457.21	819.26	746.94
Alternating Stress σ_{ea} (psi)	10394.00	898.60	0
Bending Safety Factor n	**2.53**	**34.00**	**48.82**
Torsion Safety Factor n	**1.61**	**21.89**	**28.32**

Table 6. Results of the Design Analysis of Critical Points on Shaft CD

	Keyway for Gear 2	**Step down to Gear 3 Bore Size**	**Keyway for Gear 3**	**Step by Bearing C**	**Step by Bearing D**
Ultimate Strength S_u (psi)	185500	185500	185500	185500	185500
Endurance Limit S'_n (psi)	92750	92750	92750	92750	92750
Bending Fatigue Strength S_n (psi)	52320.46	52320.46	52320.46	52320.46	52320.46
Torsion Fatigue Strength S_n (psi)	30345.86	30345.86	30345.86	30345.86	30345.86
Mean Stress σ_{em} (psi)	15149.12	19004.76	24803.37	1075.48	2361.20
Alternating Stress σ_{ea} (psi)	12030.10	12497.02	13668.45	0	0
Bending Safety Factor n	**2.82**	**2.32**	**1.83**	**48.65**	**22.16**
Torsion Safety Factor n	**1.77**	**1.44**	**1.12**	**28.22**	**12.85**

Table 7. Results of the Design Analysis of Critical Points on Shaft EF

	Keyway for Gear 4	**Step by Bearing E**	**Step by Bearing F**
Ultimate Strength S_u (psi)	90000	90000	90000
Endurance Limit S'_n (psi)	45000	45000	45000
Bending Fatigue Strength S_n (psi)	25384.59	25384.59	25384.59
Torsion Fatigue Strength S_n (psi)	14723.06	14723.06	14723.06
Mean Stress σ_{em} (psi)	5785.77	366.46	418.82
Alternating Stress σ_{ea} (psi)	17863.55	0	15147.6
Bending Safety Factor n	**2.35**	**69.27**	**5.41**
Torsion Safety Factor n	**1.69**	**40.18**	**5.08**

Table 8. Results of the Deflection Analysis on All Shafts

	Shaft AB at Gear 1	**Shaft CD**	**Shaft EF**
Maximum Deflection δ (in)	0.004	0.033 at Gear 2 0.022 at Gear 3	0.001
Rate of Twist θ/L (degrees/ft)	0.87	0.89	0.84
Critical Speed n_{crit} (rpm)	2967.28	1148	5934.56

Table 9. Results of the Key Calculations

	Key for Gear 1	**Key for Gear 2**	**Key for Gear 3**	**Key for Gear 4**
Overall Dimensions (L,W, H) (in)	0.59, 0.25, 0.25	0.82, 0.375, 0.375	0.90, 0.375, 0.375	1.58, 0.5, 0.5

4.4 Design Analysis of the Bearings

After obtaining the radial forces acting on each bearing, a simple analysis of bearing available on market catalogues can be made to determine which gears will best fit for a given application. A summary of bearing selection criteria is shown in Table 10.

Table 10. Bearing Selection

Bearing	**Load (lb)**	**Load (kN)**	**Bore (in)**	**Bore (mm)**	**Bearing**	**Bearing Max Load (kN)**	**Safety Factor (n)**
A	347.36	1.545	1.25	31.75	L06	3.35	**2.17**
B	347.36	1.545	1.25	31.75	L06	3.35	**2.17**
C	793.65	3.530	1.5	38.1	208	9.4	**2.66**
D	1143.68	5.087	1.4375	36.5125	308	10.6	**2.084**
E	653.21	2.906	1.9375	49.2125	L10	6.10	**2.099**
F	653.21	2.906	1.9375	49.2125	L10	6.10	**2.099**

Sample Calculation for Bearing A:

Given:

$D = 30mm$

$Clearance = D/1000 = 30/1000 = 0.03mm$

$Shaft\ Diameter = D - 2 * Clearance = 30 - 2 * 0.03 = 29.94mm$

The clearances and new shaft diameters needed for the bearings chosen were as follows in Table 11 and 12.

Table 11. Bearing Clearance Modifications to Shaft [5]

Bearing	**Original Shaft Bore (in)**	**Original Shaft Bore (mm)**	**Bearing Bore (mm)**	**Bearing OD (mm)**	**Clearance Bore/1000**	**New Shaft Diameter**
A L06	1.25	31.75	30 mm	55 mm	0.03 mm	29.94 mm
B L06	1.25	31.75	30 mm	55 mm	0.03 mm	29.94 mm
C 208	1.5	38.1	40 mm	80 mm	0.04 mm	39.92 mm
D 308	1.4375	36.5125	40 mm	90 mm	0.04 mm	39.92 mm
E L10	1.9375	49.2125	50 mm	80 mm	0.05 mm	49.90 mm
F L10	1.9375	49.2125	50 mm	80 mm	0.05 mm	49.90 mm

Table 12. Final Shaft Diameters in Inches for Bearing Mounting

Bearing	**Shaft Diameter (in)**
A L06	1.179 in
B L06	1.179 in
C 208	1.572 in
D 308	1.572 in
E L10	1.965 in
F L10	1.965 in

To ensure proper bearing selection, a few different factors must be taken into account. Table 10 highlights these specific properties: load, bore, and safety factor. In the scope of this design, it is important to maintain a safety factor that is in the range of 2. As mentioned above, each of the bearings will be experiencing radial loads from the shafts and must be able to carry these loads while maintaining the appropriate safety factor. The last two things to consider are the bore of the bearing and the diameter of the shaft. Minimizing the variation between these two measurements is critical. The bearings on each end of the shafts were selected according to these criteria. Additionally, to ensure that the bearing will be fitted onto the shafts with the appropriate clearance, calculations were made based on information provided from the *Clevite 77 Engine Bearings* manual. [9]

5.0 Results - Computer-Aided Designed Gear Reducer

The design analysis of the gearbox was done by treating the shafts as if they were vertically stacked in a column; however, for the ease of computer-aided design (CAD which was done with the SolidWorks software) and practical assembly, the gearbox was modelled as if the shafts were oriented horizontally in a row as illustrated in Figure 21.

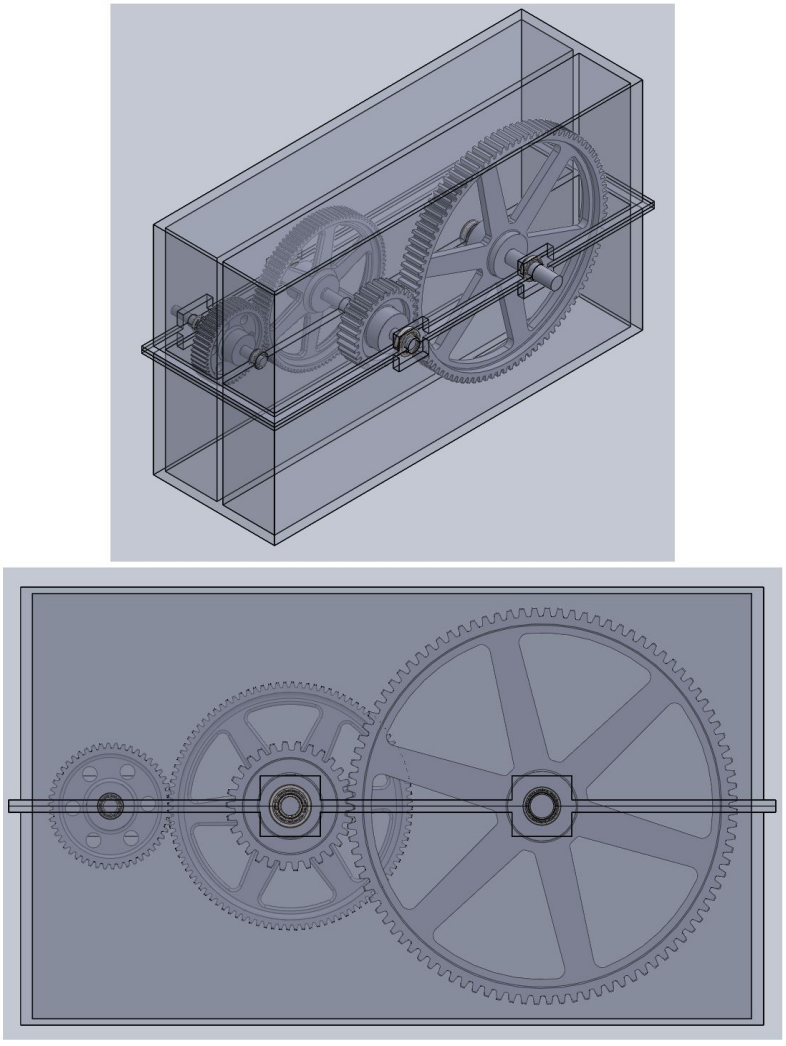

Figure 21. Gearbox CAD Model with Horizontal Shafts (Isometric View (Top of Figure 21) and Right-side View (Bottom of Figure 21))

In a vertical assembly, the loads on the shafts tend to be greater in magnitude than in a horizontal assembly as demonstrated by a vector sum bending moment diagram for the intermediate shaft in the horizontal assembly (the special case) shown in Appendix B. From the Figure A13 in the appendix, the maximum bending moment in the intermediate shaft for the special case is 418.8 lb-ft, while the maximum bending moment for the same shaft in the normal, vertical case is 476.5 lb-ft (as seen in Figure 15). Since the intermediate shaft is most prone to failure (lowest safety factor occurs in the intermediate shaft as demonstrated in Section 4.3), the gearbox would be less prone to failure if the shafts were oriented horizontally as opposed to vertically. That is to say that because the gearbox is strong enough in the vertical orientation, it is also strong enough in the horizontal orientation. Therefore, the gearbox can be oriented either horizontally or vertically when used in practicality.

The exterior walls and interior wall of the casing were designed such that each shaft has a fixed-floating bearing arrangement. Figure 22 indicates for each shaft, which bearing is axially constrained (fixed) and which bearing is axially free to move in one or both directions (floating).

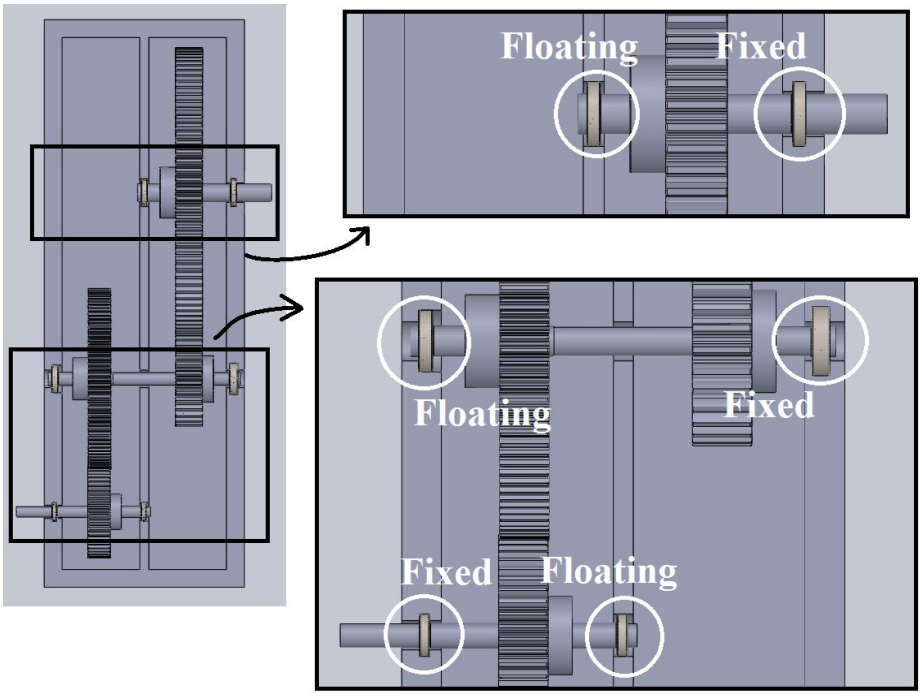

Figure 22. Identification of Fixed and Floating Bearings on Each Shaft

From the Rolling Element Bearings Presentation in the MCG 3131 - Machine Design course, the fixed-floating bearing arrangement is recommended [10]. This bearing arrangement removes a source of axial compressive stress (thus reducing this type of stress) since one bearing can freely move in the casing [11].

Figure 23 presents a drawing showing all of the gearbox components chosen in the design analysis sections; this drawing also shows that the casing has a top half and a bottom half that would be bolted together along the lips. Both halves of the casing would be sand casted.

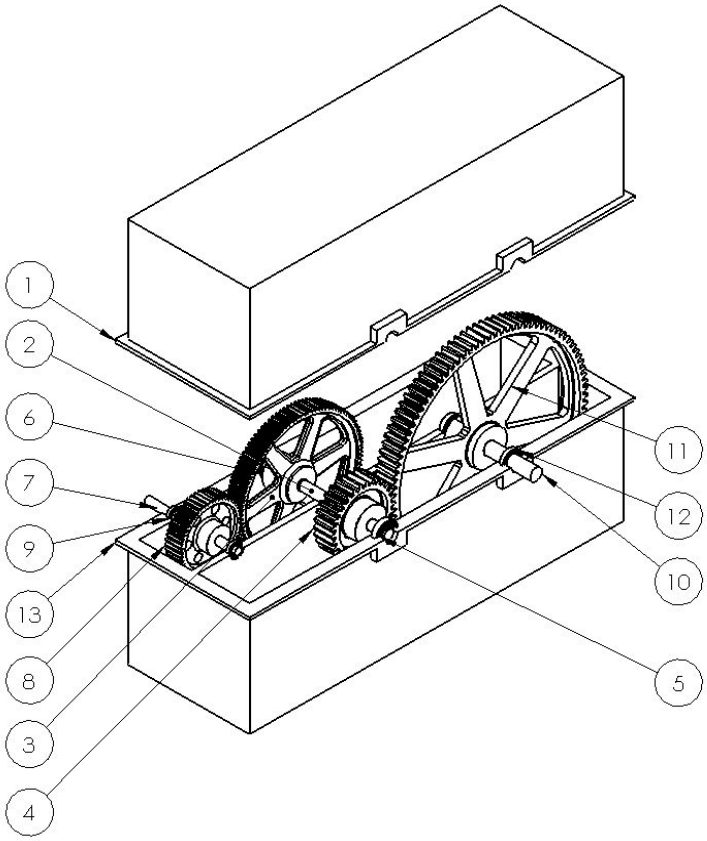

PART NUMBER	PART NAME	Quantity
1	TOP CASING	1
2	INTERMEDIATE SHAFT	1
3	GEAR YK100	1
4	GEAR NO30B	1
5	BEARING 308	1
6	BEARING 208	1
7	INPUT SHAFT	1
8	GEAR YK50	1
9	BEARING L06	2
10	OUTPUT SHAFT	1
11	GEAR NO96B	1
12	BEARING L10	2
13	BOTTOM CASING	1

Figure 23. Gearbox Components and Casing Assembly

Figure 24 shows the main dimensions of the casing; casing bearing slot clearances were each taken to be one one-thousandth of the bearing outer diameter.

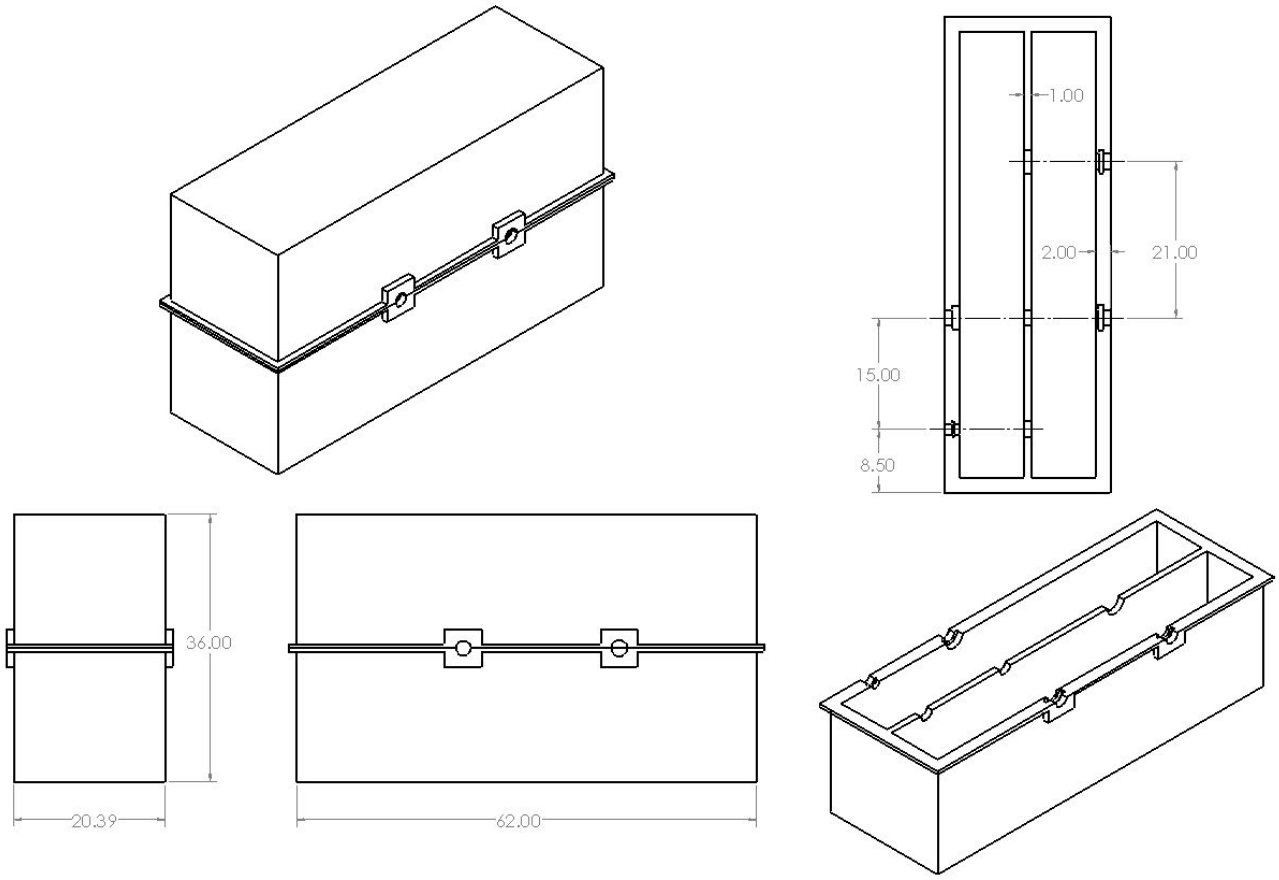

Figure 24. Main Dimensions (Inches) of the Gearbox Casing

To prevent dirt and water from entering the gearbox, a gasket would be placed in between the casing halves and v-cup seals would be inserted near the exterior faces of the bearings.

Retaining rings are sufficient for the components to be mounted on the shafts since axial forces are not expected to come from spur gears. The distances of the mounting features along the shaft, the shaft length and the shaft diameters are presented in Figures 25, 26 and 27 for the input, intermediate and output shafts respectively. For specific dimensions of the mounting features, refer to Table 3 which lists the catalog gear selections and Table 11 which lists the bearing selections from the J&M textbook.

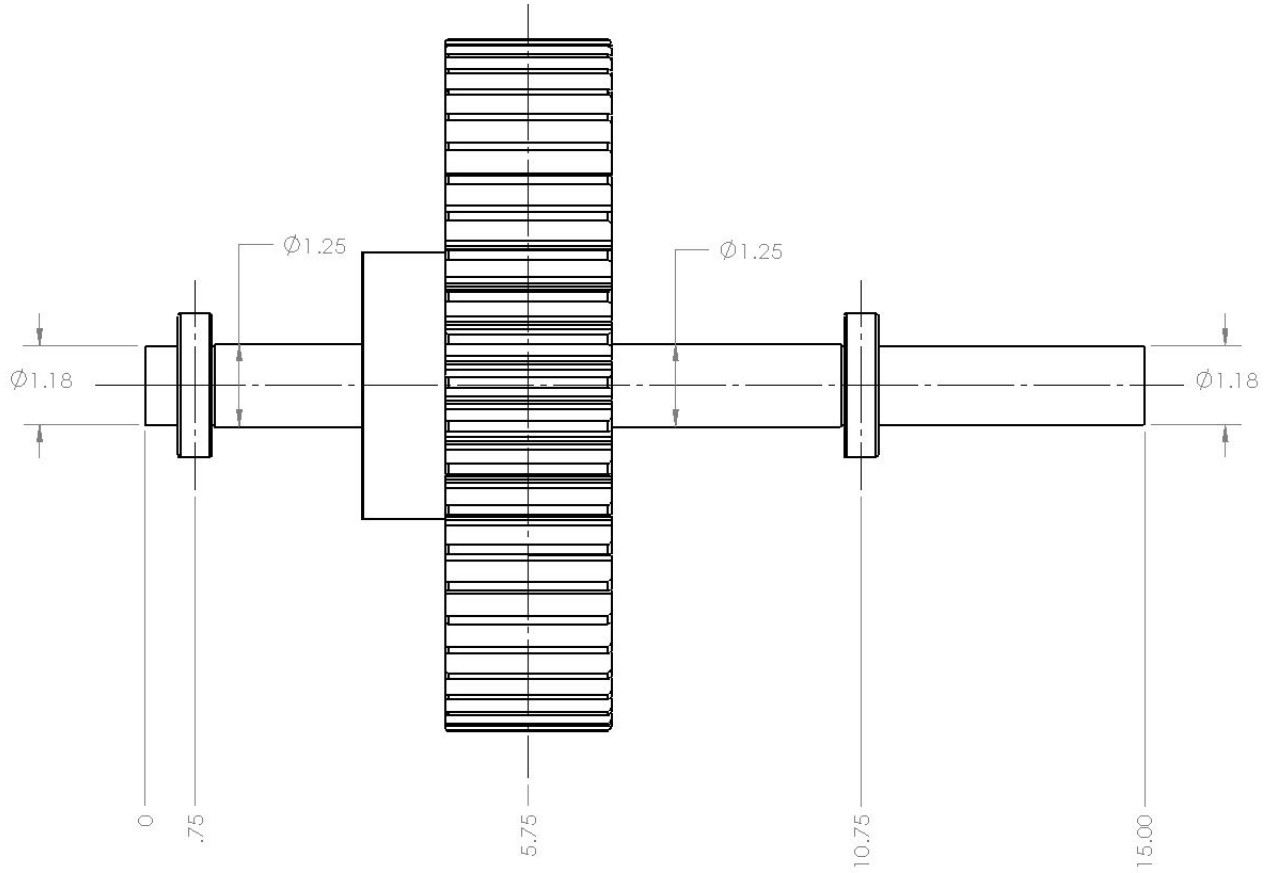

Figure 25. Location of Mounting Features on the Input Shaft and Input Shaft Dimensions (Inches)

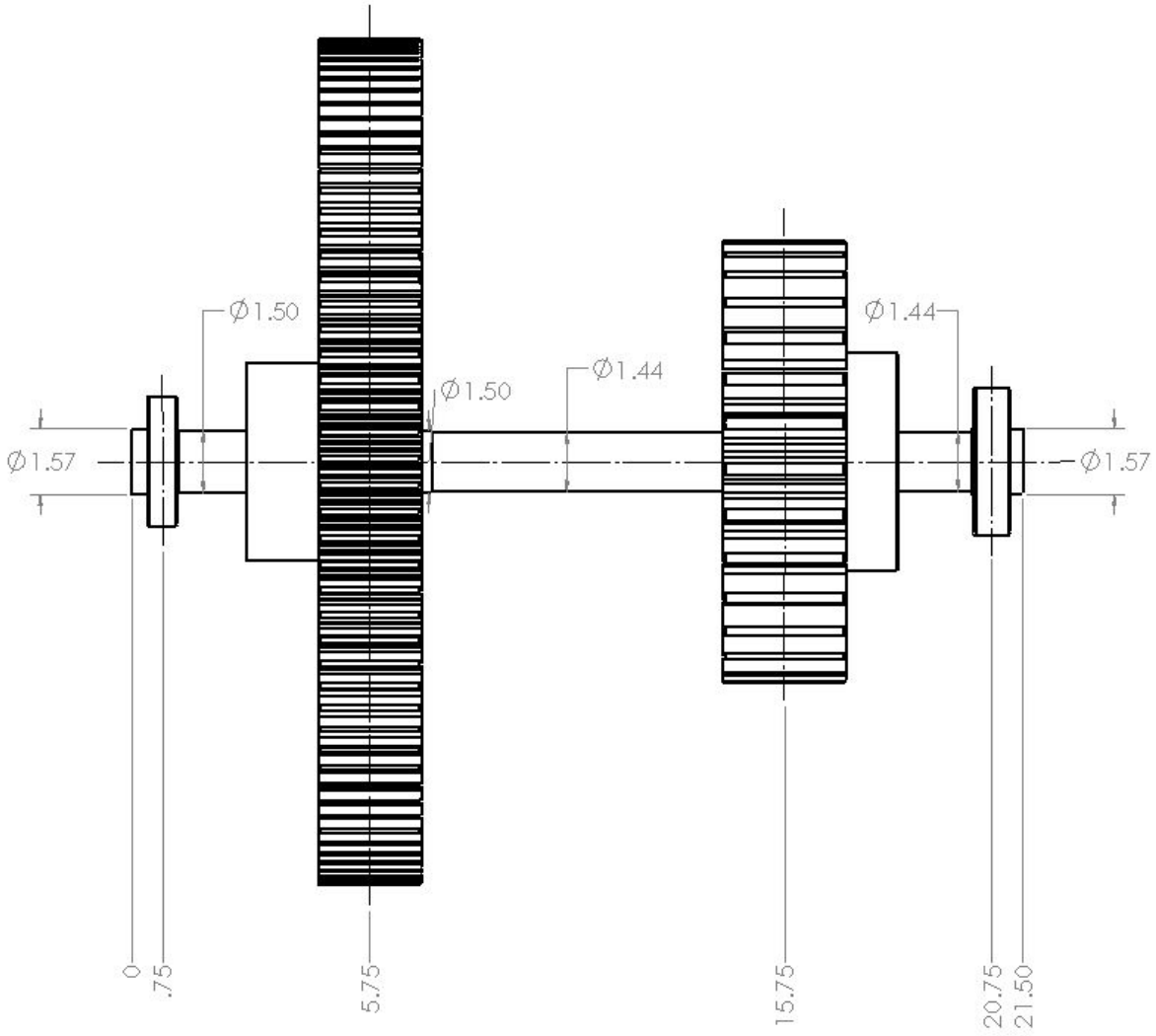

Figure 26. Location of Mounting Features on the Intermediate Shaft and Intermediate Shaft Dimensions (Inches)

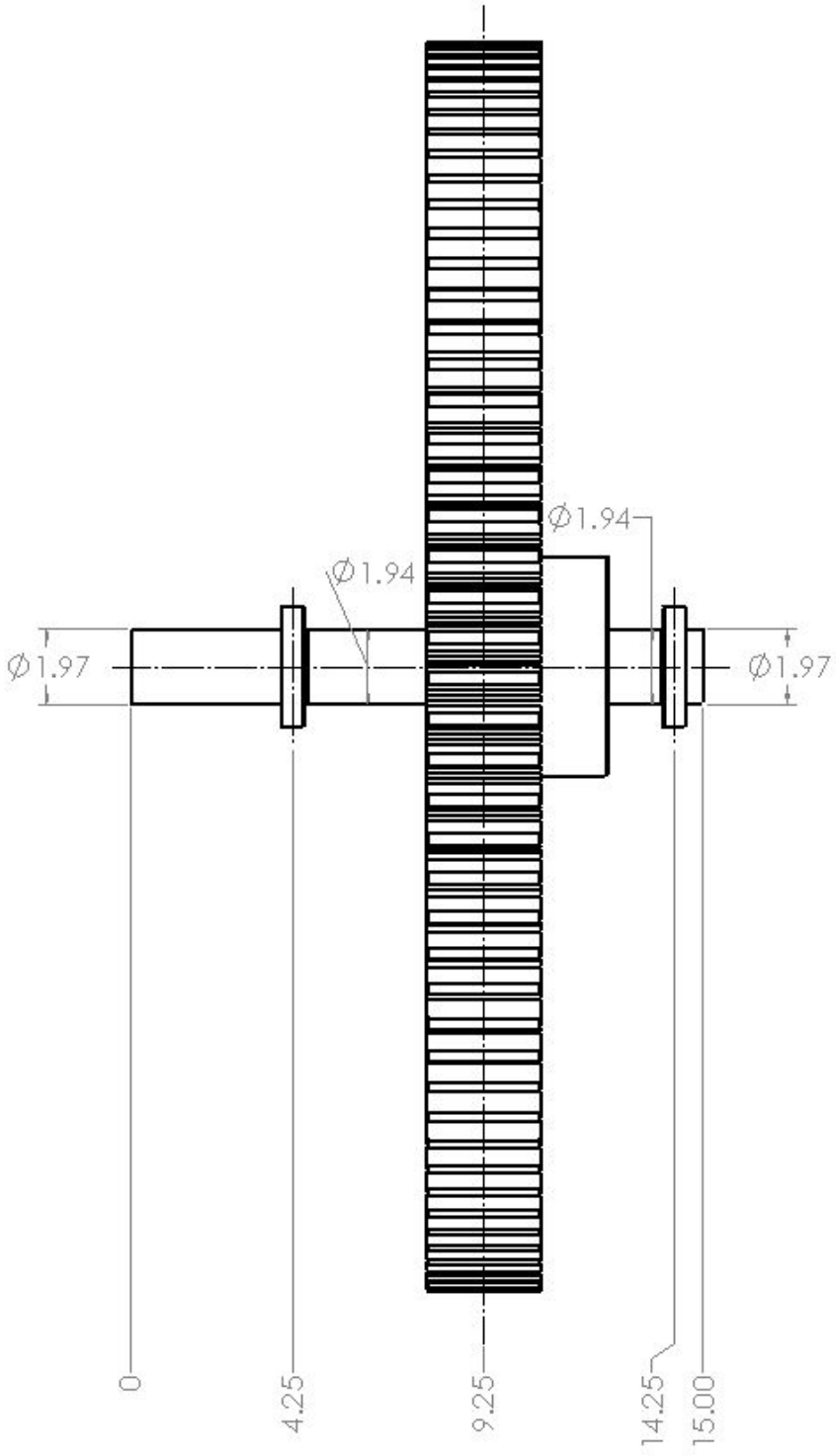

Figure 27. Location of Mounting Features on the Output Shaft and Output Shaft Dimensions (Inches)

6.0 Conclusion

The purpose of this project was for the engineering students Sharon Tam, Dan Bornstein, Osman El-Ghotmi, and Michael Botros to design a feasible and practical gear reducer given the specifications. This task required a well planned and in depth analysis of the gear reducing system, using various concepts obtained from the Machine Design Course (MCG 3131). In the preliminary stages of the design, the group conceptualized three different solutions. Once the most effective of the solutions was selected, the design process was carried out. This design process is outlined in Figure 28 below.

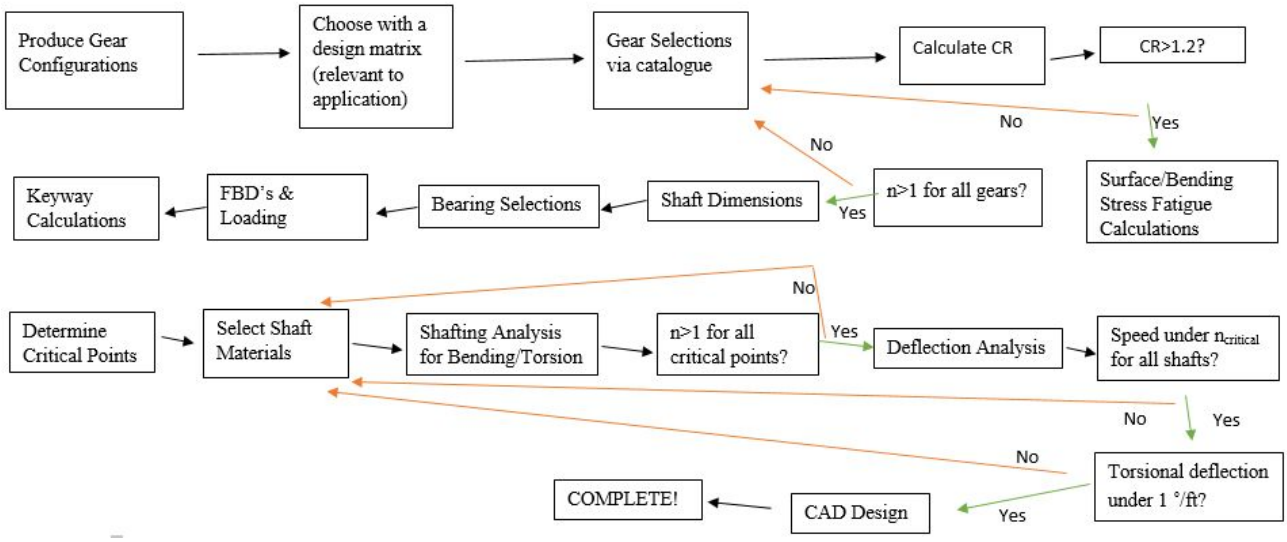

Figure 28. Design Process of the Gear Reducer

The gear reducer is to be used in Disney's commercial theme park in Florida for the drawbridge of their iconic castle; the input shaft of the gearbox is belt-driven with an electric motor and the output shaft of the gearbox is directly coupled to the drawbridge shaft. Since people would walk on this bridge, safety was one of the utmost priorities in the design analysis. The safety factors were all calculated in Section 4.0, and are summarized in Table 13 below.

Table 13: Summary of Safety Factors

Bending Stress Fatigue						
Safety Factor *n*	**Gear 1**	**Gear 2**	**Gear 3**	**Gear 4**		
	1.15	1.28	1.31	1.46		
Surface Stress Fatigue						
Safety Factor *n*	**Gear 1**	**Gear 2**	**Gear 3**	**Gear 4**		
	1.49	1.56	1.31	1.37		
Shaft AB Critical Points						
Safety Factor *n*	**Keyway for Gear 1**	**Step by Bearing A**	**Step by Bearing B**			
Bending	2.53	34.00	48.82			
Torsion	1.61	21.89	28.32			
Shaft CD Critical Points						
Safety Factor *n*	**Keyway for Gear 2**	**Step down to Gear 3 Bore Size**	**Keyway for Gear 3**	**Step by Bearing C**	**Step by Bearing D**	
Bending	2.82	2.32	1.83	48.65	22.16	
Torsion	1.77	1.44	1.12	28.22	12.85	
Shaft EF Critical Points						
Safety Factor *n*	**Keyway for Gear 4**	**Step by Bearing E**	**Step by Bearing F**			
Bending	2.35	69.27	5.41			
Torsion	1.69	40.18	5.08			
Bearing Load						
Safety	**Bearing A**	**Bearing B**	**Bearing C**	**Bearing D**	**Bearing E**	**Bearing F**

Factor *n*	2.17	2.17	2.66	2.084	2.099	2.099

The safety factors in the regions of high stress are in the range of $\mathbf{1 < n \leq 3}$, meaning that the gearbox design is reliable. Even though some of the safety factors are large, those are the safety factors associated with stress concentrators near the shaft ends where the stresses are low (the steps were successfully chosen at locations of low stress). Moreover, the two-halves, bolted casing design allows for the gearbox to be easily assembled, so the design would score high in the maintenance criterion. Ultimately, this gearbox, with laterally offset input and output shafts, will perform well at taking an input power of 5 Hp to convert a input rotation speed of 100 rpm to an output rotation speed of 15 rpm.

7.0 References

[1] Ahmed, A. F., Dr. (n.d.). *Gearing Presentation* [Slideshow].

[2] *Ball and roller bearings*. (1997). Osaka, Japan: NTN Corporation.

[3] Boston Gear offers the industry's largest line up of reliable speed reducers, gearing and other quality drivetrain components. (n.d.). Retrieved from https://www.bostongear.com/

[4] Horizontal Shaft Mixer. (n.d.). Retrieved from http://www.mixersystems.com/product/horizontal-shaft-mixer/#fndtn-panel2-1

[5] Juvinall, R. C., & Marshek, K. M. (2017). *Fundamentals of machine component design*. Hoboken, NJ: John Wiley & Sons.

[6] *Geometry factors for determining the pitting resistance and bending strength of spur, helical and herringbone gear teeth*. (1989). Alexandria, VA: American Gear Manufacturers Association.

[7] François, R., Dr. (n.d.). *MCG 2101 Intro to Design Lecture 4* [Slideshow].

[8] AISI 3140. (2018). Retrieved July 22, 2018, from http://www.matweb.com/search/datasheet.aspx?MatGUID=0f434bedc44b446ea567082ca912a5d6

[9] HOW MUCH CLEARANCE DO YOUR BEARINGS NEED? (2005, February 14). Retrieved July 22, 2018, from https://www.mahle-aftermarket.com/media/local-media-north-america/pdfs/cl77-1-205r.pdf

[10] Ahmed, A. F., Dr. (n.d.). *Rolling elements bearing Presentation* [Slideshow].

[11] Design of bearing arrangements. (n.d.). Retrieved July 22, 2018, from https://medias.schaeffler.com/medias/en!hp.tg.cat/tg_hr*ST4_1652155275

Appendix A - Report Contribution of Each Team Member

An outline of how each team member contributed to this report is presented in Table A1.

Table A1. Detailed Report Contribution of the Group of Four Members

Team Member	Specific Contribution
Sharon Tam	● Planning of Solution 1 ● Gear selection calculations (max and min teeth, gear ratios) and selection of gears, and writing out the process in the report ● Table with final gear choices ● Surface Stress Fatigue calculations ● Shaft Calculations for AB (S.F for Bending and Torsion, Angle of Twist, Critical Speed) at all the critical points (Keyway, steps to accommodate bearings) ● Minimum keyway length calculations for Gear 1 and 2. ● Creating excel sheets on calculations done above to make recalculating values easier ● Obtaining CAD files for the gears and bearings from Boston Gear's website and Solidworks Toolbox respectively. Requested any missing CAD files from Boston Gear ● Typed out sample calcs for the gear interference, gear fatigue analysis, keyway length, and formatted all the sample calcs to be uniform ● Formatted the equations in the report and explained how they are used ● Tabulated calculation results in the report
Dan Bornstein	● Write out of the decision matrix and definitions of the selection criteria and weight values for these criteria. ● Wrote out process in filling in decision matrix and choosing the solution 1 based on the decision matrix ● Bending stress fatigue calculations for gears 1 and 2 ● Contact ratio calculations for gears 1 and 2 ● Shaft Calculations for EF (S.F for Bending and Torsion, Angle of Twist, Critical Speed) ● Min. keyway length calculations for Gear 3 and 4. ● Bearing clearance analysis ● Shafting analysis for steps (change in d) at the interfaces of

	bearings to find safety factors ○ Determining kt, kts, q, qs, kf, kfs, based of the larger and smaller shaft diameters at step, and the chosen fillet radius of 0.2 in ● Assisted in writing the sample calculations in the report ● Assisted in producing the shafts for the CAD assembly ● Wrote out the explanation of the decision process and assumptions made throughout the design steps ● Designed the flow chart to outline the design process in the conclusion
Osman El-Ghotmi	● Abstract ● Introduction ● Incorporation of gear reducer (Part of the Theoretical Background) ● Planning Solution 3 with Michael ● Shaft FBD's ● Calculated the Shaft Reaction Forces at the bearing ends and the wrote description of work. ● Conducted the Design Analysis of the Bearings by using the radial loads and shaft diameters to select appropriate catalogue bearings and the description of work. ● Determining Shaft Steps for bearing selections with Dan. ● Created the tables and calculated the clearances for the shaft diameters. ● Wrote the description for the procedure involved in determining contact ratio, bending stresses, surface fatigue, and their corresponding safety factors. ● Calendar
Michael Botros	● Overall report plan and analysis plan ● Delegation of tasks ● Theoretical Background: purpose of a gear reducer, context of this project's gear reducer ● Generation of Solutions: write-up describing the purpose of generating solutions and drawing of Solution 3 ● Decision Matrix: creation of the table ● Design Analysis Approach and Assumptions: added to what Dan previously wrote there ● Selection of Specific Gears and Bearings types: typed speed ratio equations and procedure for catalog selection ● Design Analysis of the Gears: bending safety factor calculation

	for gears 3 and 4 meshing ● Design Analysis of the Shafts: ○ Worked with Sharon to review Osman's equilibrium calculations ○ used SkyCiv to produce shaft free-body diagrams ○ Collaborated with team mates to decide on shaft lengths, casing dimensions, the location and the size of the step radius on shaft CD ○ Typed up method and equations for creating shear force, bending moment and torsion diagrams, used SkyCiv to produce those diagrams for all shafts ○ Calculation of bending and torsion safety factors for three critical points on shaft CD, angle of twist calculation for shaft CD, calculations for its deflection and critical speed ○ Typed keyway equations (to add to Sharon's key design write-up) ● Results - Computer-Aided Designed Gear Reducer: ○ Description of model with pictures ○ Fixed-floating bearing arrangements ○ Gearbox drawing with all components including casing ○ Casing drawings ○ Shaft drawings with mounting features ● Conclusion: justification of the design ● Proof-reading of entire report

Appendix B - Additional Load Diagrams for the Shafts

For all of the shafts, the shear force and bending moment diagrams in the xy and xz planes are presented in Figures B1 to B12; all load diagrams were generated with the SkyCiv engineering software.

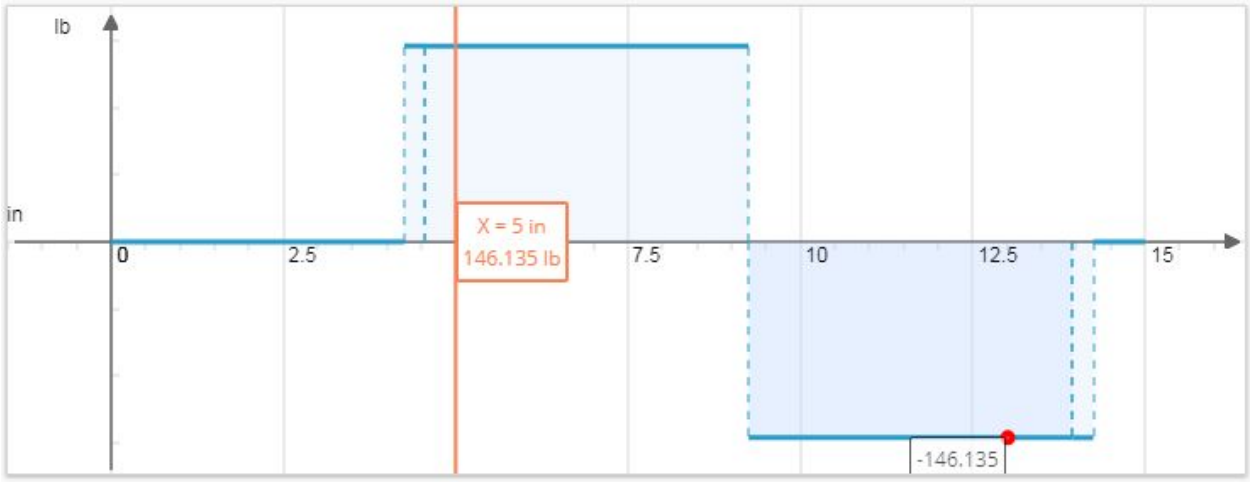

Figure B1. Shear Force in the x-y Plane as a Function of Distance x along the Input Shaft

Figure B2. Shear Force in the x-z Plane as a Function of Distance x along the Input Shaft

Figure B3. Bending Moment in the x-y Plane as a Function of Distance x along the Input Shaft

Figure B4. Bending Moment in the x-z Plane as a Function of Distance x along the Input Shaft

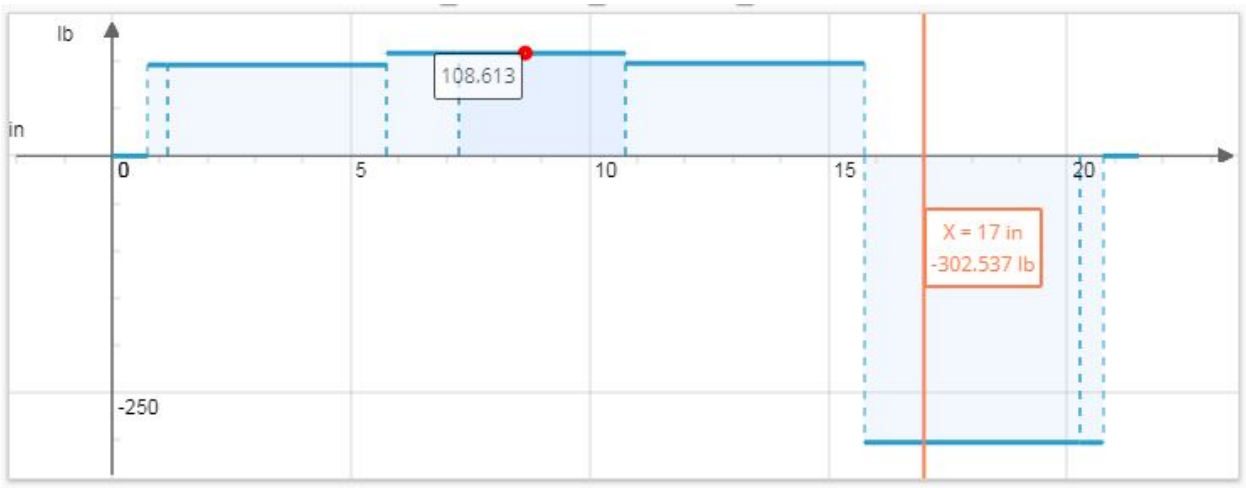

Figure B5. Shear Force in the x-y Plane as a Function of Distance x along the Intermediate Shaft

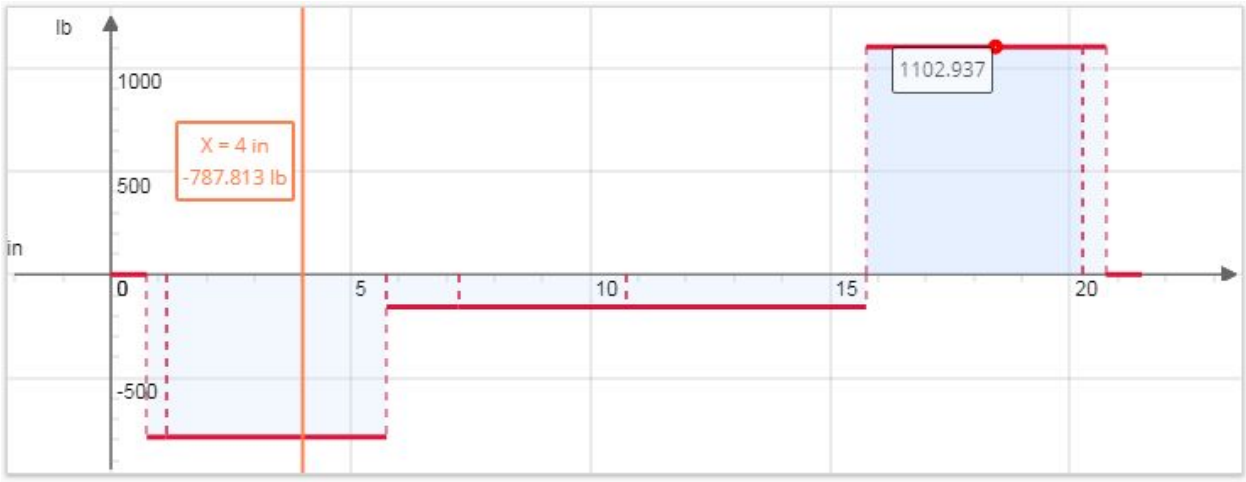

Figure B6. Shear Force in the x-z Plane as a Function of Distance x along the Intermediate Shaft

Figure B7. Bending Moment in the x-y Plane as a Function of Distance x along the Intermediate Shaft

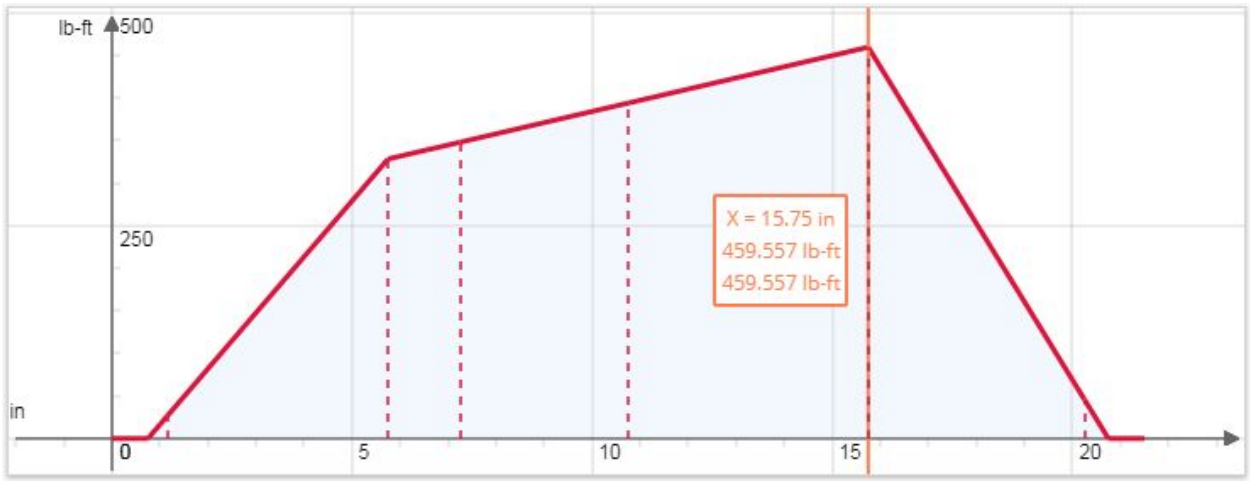

Figure B8. Bending Moment in the x-z Plane as a Function of Distance x along the Intermediate Shaft

Figure B9. Shear Force in the x-y Plane as a Function of Distance x along the Output Shaft

Figure B10. Shear Force in the x-z Plane as a Function of Distance x along the Output Shaft

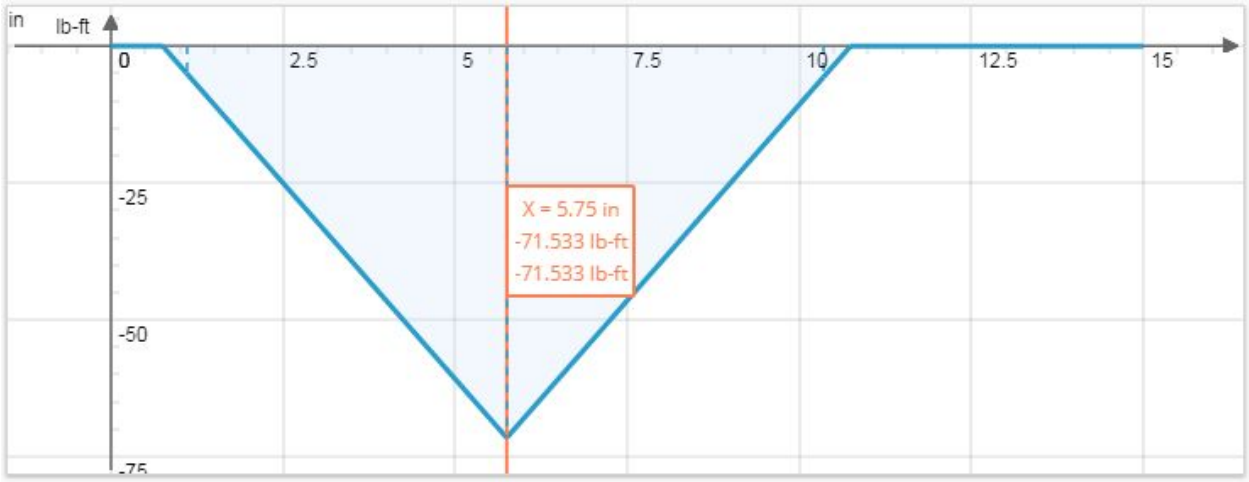

Figure B11. Bending Moment in the x-y Plane as a Function of Distance x along the Output Shaft

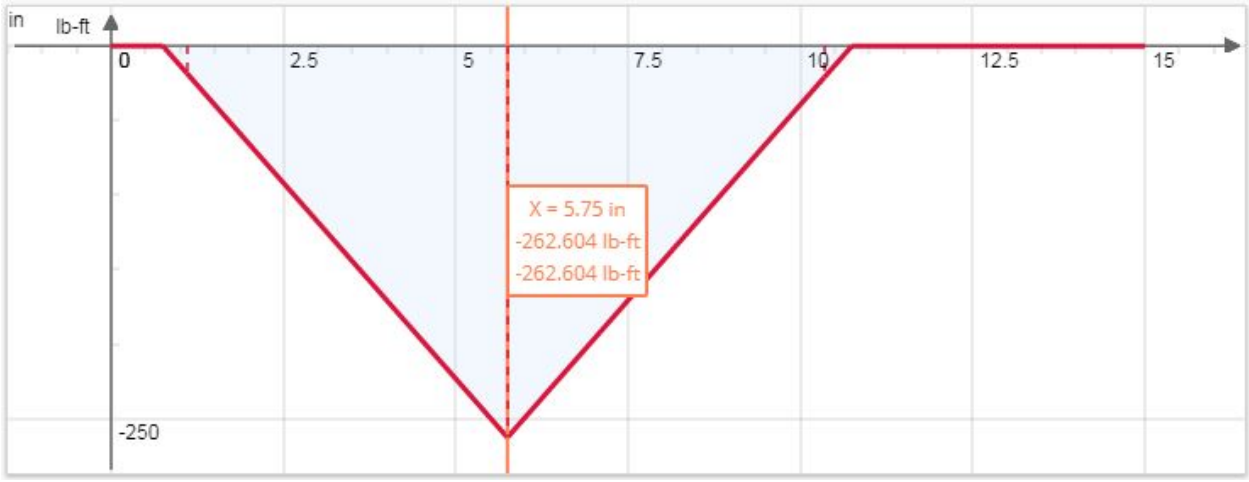

Figure B12. Bending Moment in the x-z Plane as a Function of Distance x along the Output Shaft

The vector sum bending moment diagram for the intermediate shaft is presented in Figure B13 considering the special case (shafts oriented horizontally instead of vertically).

Figure B13. Special Case (Horizontal Shafts) - Vector Sum of the Bending Moment as a Function of Distance x along the Intermediate Shaft

Appendix C - Sample Calculations

C-1 - Gear Interference Check

An example of the calculations done to determine the minimum pinion teeth, and the maximum gear teeth to prevent gear interference are shown below. The same calculations were used to find the minimum pinion teeth in gear 1, but in gear 2, since the pressure angle is 20°, any pinion with more than 18 teeth (the pinion has 50 teeth), will not interfere with any number of gear teeth. [5 and 7]

Knowns for Gear 3 and 4:

$$k = 1 \qquad R = \frac{10}{3} \qquad \phi = 14.5°$$

Minimum Pinion Teeth for Gear 3:

$$N_p = \frac{2k}{(1+2R\sin^2\phi}\left(R + \sqrt{R^2 + (1+2R)\sin^2\phi}\right)$$

$$= \frac{2(1)}{(1+2(10/3))sin^2(14.5°)}\left((\frac{10}{3}) + \sqrt{(\frac{10}{3})^2 + (1+2(\frac{10}{3}))sin^2(14.5°)}\right)$$

$N_p = 28.04 \simeq 29\ teeth$

Maximum Gear Teeth for Gear 4 if Gear 3 has 30 teeth:

$$N_g = \frac{N_p^2 sin^2\phi - 4k^2}{4k - 2N_p sin^2\phi} = \frac{(30)^2 sin^2(14.5°) - 4(1)^2}{4(1) - 2(30)sin^2(14.5°)} = 219.70\ teeth \simeq 220\ teeth$$

C-2 - Gear Loading and Fatigue

Samples of the final calculations of the gear fatigue analysis are shown below. They encompass the contact ratio, and the failure modes of bending and surface fatigue.

Knowns for Gear 1 and 2:

$N_p = 50 \qquad d_p = 10\ in \qquad b_p = 2.5\ in \qquad N_g = 100 \qquad d_g = 20\ in \qquad b_g = 2.5\ in$

$\phi = 20° \qquad P = 5\ in \qquad p = \frac{\pi}{P} = \frac{\pi}{5} = 0.628\ in \qquad t = \frac{p}{2} = 0.314\ in$

$r_{bp} = r_p cos(\phi) = \frac{10}{2} cos(20°) = 4.698\ in \qquad r_{bg} = r_g cos(\phi) = \frac{20}{2} cos(20°) = 9.397\ in$

$p_b = pcos(\phi) = 0.628 cos(20°) = 0.5901\ in$

$H = 5\ hp \qquad n = 100\ rpm$

$V = \frac{\pi d_p n}{12} = \frac{\pi(10)(100)}{12} = 261.8\ ft/min$

$F_t = \frac{33000H}{V} = \frac{33000(5)}{261.8} = 630.25\ lbf$

$R = 2$

$I = \frac{sin\phi cos\phi}{2} \cdot \frac{R}{R+1} = \frac{sin(20°)cos(20°)}{2} \cdot \frac{2}{1+2} = 0.1071$

Contact Ratio (CR) for Gear 1 and 2:

$$CR = \frac{\sqrt{(r_p+P^{-1})^2 - r_p^2 cos^2\phi} + \sqrt{(r_g+P^{-1})^2 - r_g^2 cos^2\phi} - (r_p+r_g)sin\phi}{p_b}$$

$$= \frac{\sqrt{(5+5^{-1})^2 - 5^2 cos^2(20°)} + \sqrt{(10+5^{-1})^2 - 10^2 cos^2(20°)} - (5+10)sin(20°)}{0.5901}$$

$$CR = 1.805 > 1.2 \; acceptable$$

Bending Stress Fatigue for Gears 1 (pinion) and 2 (gear):

For ASTM class 30 gray cast iron from Appendix C-3a [5]:

$$S_u = 31 \; ksi \qquad S'_n = 0.5S_u = 15.5 \; ksi$$

From Table 8.1 and Figure 8.13 of the textbook:

$$C_L = 1 \qquad C_G = 0.85 \qquad C_s = 1 \qquad k_r = 0.814 \qquad k_t = 1 \qquad k_{ms} = 1.4$$

$$S_n = S'_n C_L C_G C_s k_r k_t k_{ms} = (15.5)(1)(0.85)(1)(0.814)(1)(1.4) = 15.014 \; ksi$$

From Figure 15.23 of the textbook (For the gears with pressure angle of 14.5°, the AGMA-908-B39 information sheet) [5 and 6]:

$$J_p = 0.28 \qquad J_g = 0.31$$

From Figure 15.24, Table 15.1, and Table 15.2 respectively textbook [5]:

$$K_v = \frac{600+V}{600} = \frac{600+261.8}{600} = 1.436$$

$$K_o = 1.25$$

$$K_m = \frac{2.5-2}{6-2}(1.7 - 1.6) + 1.6 = 1.6125$$

$$\sigma_p = \frac{F_t P}{bJ_p} K_v K_o K_m = \frac{(630.25)(5)}{(2.5)(0.28)}(1.436)(1.25)(1.6125) = 13033.22 \; psi$$

$$\sigma_g = \frac{F_t P}{bJ_g} K_v K_o K_m = \frac{(630.25)(5)}{(2.5)(0.31)}(1.436)(1.25)(1.6125) = 11771.95\ psi$$

$$n_p = \frac{S_n}{\sigma_p} = \frac{15014}{13033.22} = 1.15 > 1\ acceptable$$

$$n_g = \frac{S_n}{\sigma_g} = \frac{15014}{11771.95} = 1.28 > 1\ acceptable$$

Surface Fatigue for Gears 1 (pinion) and 2 (gear):

For ASTM class 30 gray cast iron from Appendix C-3a of the textbook [5]: $S_{fe} = 70\ ksi$

From Figure 15.27 of the textbook [5]:

$\#cycles\ pinion = 10^7 cycles$ $\qquad C_{Lip} = 1.0$

$\#cycles\ gear = \frac{50}{100}(10^7) = 5 \times 10^6 cycles$ $\qquad C_{Lig} = 1.05$

From Table 15.6 of the textbook [5]:

$C_R = 1.0$ (99% reliability)

$$S_{Hp} = S_{fe} C_{Lip} C_R = (70)(1.0)(1.0) = 70\ ksi$$

$$S_{Hg} = S_{fe} C_{Lig} C_R = (70)(1.05)(1.0) = 73.5\ ksi$$

From Table 15.4a of the textbook [5]:

$C_P = 1800\ \sqrt{psi}$

$$\sigma_H = C_p \cdot \sqrt{\frac{F_t}{bd_p I} K_v K_o K_m} = 1800 \cdot \sqrt{\frac{630.25}{(2.5)(10)(0.1071)}(1.436)(1.25)(1.6125)}$$

$$\sigma_H = 46982.31\ psi$$

$$n_p = \frac{S_{Hp}}{\sigma_H} = \frac{70000}{46982.31} = 1.49 > 1 \; acceptable$$

$$n_g = \frac{S_{Hg}}{\sigma_H} = \frac{70000}{46982.31} = 1.56 > 1 \; acceptable$$

C-3 - Free-Body Diagram Analysis of the Reaction Forces

The reaction forces for each shaft are calculated below. The analysis for each shaft is different, thus all the calculations are shown.

Calculations for Shaft AB:

$$V_1 = \frac{\pi d_1 n_1}{12} = \frac{\pi(10)(100)}{12} = 261.80 \, fpm$$

$$F_{t1} = \frac{33000(H)}{V} = \frac{33000(5)}{261.80} = 630.25 \; lbf$$

$$F_{r1} = F_{t1} tan(\phi_1) = (630.25)(tan(20)) = 229.39 \; lbf$$

$$W_{G1} = 57.66 \; lbf$$

$$W_{S1} = 5.2175 \; lbf$$

$$W_1 = 57.66 + 5.2175 = 62.8775 \; lbf$$

X-Y:

$\Sigma M_A = 0 : \ (10)B_y + (5)(-229.39 - 62.8775) = 0 \Rightarrow B_y = 146.13375 \ lbf$

$\Sigma F_y = 0 : \ Ay - 229.39 - 62.8775 + 146.13375 = 0 \Rightarrow B_z = 146.13375 \ lbf$

X-Z:

$\Sigma M_A = 0 : \ -(10)B_z + (5)(630.25) = 0 \Rightarrow B_z = 315.125 \ lbf$

$\Sigma F_y = 0 : \ Az - 620.25 + 315.125 = 0 \Rightarrow A_z = 315.125 \ lbf$

$A_r = (A_y{}^2 + A_z{}^2)^{1/2} \Rightarrow A_r = 347.36 \ lbf$

$B_r = (B_y{}^2 + B_z{}^2)^{1/2} \Rightarrow B_r = 347.36 \ lbf$

Calculations for Shaft CD:

$F_{r2} = F_{r1} = 229.39 \ lbf$

$F_{t2} = F_{t1} = 630.25 \ lbf$

$T_2 = F_{t2}(\frac{d_2}{2}) = (630.25)(\frac{20}{2})$

$W_{G2} = 216.88 \ lbf$

$W_{G3} = 74.37 \ lbf$

$W_{S2} = 10.7675 \ lbf$

$\Sigma T = 0 : T_3 = T_2 = 6302.5 \ lb - in$

$F_{t3} = \frac{F_3}{d_3/2} = \frac{6302.5}{10/2} = 1206.5 \ lbf \Rightarrow 1260.5 \ lbf$

$F_{r3} = F_{t3} tan(\phi_3) = (1260.5) tan(14.5) = 325.99 \ lbf$

X-Y:

$$\Sigma M_c = 0: \ (5)(229.39) - (10)(10.7675) - (5)(216.88) - 15(325.99) - (15)(74.37) + (20)D_y = 0 \Rightarrow D_y = 302.53 \ lbf$$

$$\Sigma F_y = 0: \ C_y + 229.39 - 216.88 - 10.7675 - 74.37 - 325.99 + 302.53 = 0$$

$$C_y = 96.0875 \ lbf$$

X-Z:

$$\Sigma M_c = 0: \ -(5)(630.25) - (15)(1260.5) - (20)D_z = 0 \Rightarrow D_z = -1102.94 \ lbf$$

$$\Sigma F_z = 0: \ C_z + 630.25 + 1260.5 - 1102.94 = 0 \Rightarrow C_z = 787.81 \ lbf$$

$$C_r = (C_y^2 + C_z^2)^{1/2} \Rightarrow C_r = 793.65 \ lbf$$

$$D_r = (D_y^2 + D_z^2)^{1/2} \Rightarrow D_r = 1143.68 \ lbf$$

Calculations for Shaft EF:

$$F_{r4} = F_{r3} = 325.99 \ lbf$$

$$F_{t4} = F_{t3} = 1260.5 \ lbf$$

$$W_{G4} = 656.82 \ lbf$$

$$W_{S3} = 12.5325 \ lbf$$

$$W_4 = 669.3525 \ lbf$$

X-Y:

$$\Sigma M_D = 0: \ (5)(325.99 - 669.3525) + (10)F_y = 0 \Rightarrow F_y = 171.68125 \ lbf$$
$$\Sigma F_y = 0: \ E_y + 325.99 - 669.35253 + 171.68125 = 0 \Rightarrow E_y = 171.68125 \ lbf$$

X-Z:

$$\Sigma M_D = 0: \ + (5)(1260.5) - (10)F_z = 0 \Rightarrow F_z = 630.25 \ lbf$$
$$\Sigma F_z = 0: \ E_z - 1260.5 + 630.25 = 0 \Rightarrow E_z = 630.25 \ lbf$$

$$F_r = (F_y{}^2 + F_z{}^2)^{1/2} \Rightarrow F_r = 653.21 \ lbf$$
$$E_r = (E_y{}^2 + E_z{}^2)^{1/2} \Rightarrow E_r = 653.21 \ lbf$$

$$V_1 = \frac{33000H}{F_{t4}} = \frac{33000(5)}{1260.5} = 130.9 \ fpm$$
$$n_4 = \frac{12V_4}{\pi d_4} = \frac{12(130.9)}{\pi(32)} = 15.625 \ rpm$$
$$T_o = T_4 = F_{t4}\frac{d_4}{2} = (1260.5)(\tfrac{32}{2}) = 20168 \ lb - in$$

C-4 - Shaft Stress Safety Factor Analysis

The shaft analysis calculations for a critical point 1.5 inches from gear 2 on shaft CD is shown below as sample calculations. The other shafts were analyzed in a similar fashion where applicable.

Using SkyCiv, the maximum bending moment and torque at this point were 4242.552 lb-in and 6302.5 lb-in, respectively.

Knowns for the Shaft (alternating reversing bending, and constant torque):

$$M_a = 4224.696\ lb-in,\ M_m = 0,\ T_a = 0,\ T_m = 6302.5\ lb-in$$

For 4340 Normalized Steel in Appendix C-4a [5]:

$$S_u = 185.5\ ksi$$

$$S_n' = 0.5S_u = 0.5 * 185.5 = 92.75\ ksi$$

Bending Endurance Limit Calculations:

From Table 8.1 of the textbook [5]:

$$C_L = 1$$

$$C_G = 0.9 \quad (d = 1.4375\ in,\ 0.4 < 1.4375 < 2)$$

$$C_T = 1 \quad (\text{since } T < 840\ ^\circ F)$$

$$C_R = 0.814 \quad (99\%\ \text{reliability})$$

From Figure 8.13 of the textbook [5]:

$$C_S = 0.77 \quad \text{for machined shafts}$$

$$S_n = S_n' C_L C_G C_S C_T C_R$$

$$S_{n-bending} = (45 \times 10^3)(1)(0.9)(0.77)(1)(0.814) = 25384.59\ psi$$

Torsional Endurance Limit Calculations:

$$S_n = S_n' C_L C_G C_S C_T C_R$$

From Table 8.1 of the textbook [5]:

$C_L = 0.58$

All other constants remain the same

$S_{n-torsion} = (45 \times 10^3)(0.58)(0.9)(0.77)(1)(0.814) = 14723.0622\ psi$

Calculating stress concentration factors for the step of the shaft with a fillet radius of 1/32 in.:

$D = 1.5in,\ d = 1.4375in,\ r = \frac{1}{32}in$

$\frac{r}{d} = \frac{\frac{1}{32}}{1.4375} = 0.02174in$

$\frac{D}{d} = \frac{1.5}{1.4375} = 1.043in$

Using Figure 4.35 in the textbook [5]:

$K_t = 2.03$ for bending

$K_{ts} = 1.45$ for torsion

Using Figure 8.24 [5]:

$q = 0.7,\ q_s = 0.75$

Calculating the final stress concentration factors:

$K_f = 1 + (K_t - 1)q = 1 + (2.03 - 1) * 0.7 = 1.721$

$K_{fs} = 1 + (K_{ts} - 1)q = 1 + (1.45 - 1) * 0.75 = 1.3375$

Calculating alternating and median stresses:

$$\sigma_{ea} = \frac{16}{\pi d^3}\sqrt{4K_f M^2{}_a + 3K_{fs} T_a{}^2}$$

$$= \frac{16}{\pi 1.4375^3}\sqrt{4 * 1.721 * 4224.696 + 3 * 1.3375 * 0} = 19004.76239\ psi$$

$$\sigma_{em} = \frac{16}{\pi d^3}(K_f M_m + \sqrt{K_f M^2{}_m + K_{fs} T_m{}^2})$$

$$= \frac{16}{\pi 1.4375^3}(1.721 * 0 + \sqrt{1.721 * 0 + 1.3375 * 6302.5^2} = 12497.01524\ psi$$

Calculating safety factors using Modified Goodman Criteria:

$$\frac{\sigma_{ea}}{S_n} + \frac{\sigma_{em}}{S_u} = \frac{1}{n}$$

$$n = \frac{S_n S_u}{\sigma_{ea} S_u + \sigma_{em} S_n}$$

$$n_{bending} = \frac{52320.4605 * 185500}{19004.76239 * 185500 + 12497.01524 * 52320.4605} = 2.32 > 1\ acceptable$$

$$n_{torsion} = \frac{30345.86709 * 185500}{19004.76239 * 185500 + 12497.01524 * 30345.86709} = 1.44 > 1\ acceptable$$

Calculating the Torsional Deflection of Shaft CD:

$$\theta = \Sigma \frac{32TL}{\pi G d^4} = \frac{32T}{\pi G}\left(\frac{L_1}{d_1^4} + \frac{L_2}{d_2^4}\right) = \frac{32}{\pi(11300 \times 10^3)}\left(\frac{1.5}{1.5^4} + \frac{8.5}{1.4375^4}\right) = 0.01299\ rad = 0.744°$$

$$\frac{\theta}{\Sigma L} = \frac{\theta}{L_1 + L_2} = \frac{0.744°}{1.5 + 8.5} = 0.0744°/in = 0.8933°/ft < 1°/ft\ acceptable$$

Calculating the Critical Speed of Shaft CD:

The displacements at each gear was computed using SkyCiv and verified.

$\delta_1 = 0.03287\ in$ $\quad \delta_2 = 0.02243\ in$

$w_1 = 630.37\ lb$ $\quad w_2 = 1322.55\ lb$

$g = 386.04\ in/s^2$

For shaft CD, the configuration has multiple masses. Thus, from Figure 17.5 in the textbook [5]:

$$n_{crit} = \frac{30}{\pi}\sqrt{\frac{g\Sigma w\delta}{\Sigma w\delta^2}} = \frac{30}{\pi}\sqrt{\frac{g(w_1\delta_1+w_2\delta_2)}{(w_1\delta_1^2+w_2\delta_2^2)}} = \frac{30}{\pi}\sqrt{\frac{(9.81)((630.37)(0.03287)+(1322.55)(0.02243))}{((630.37)(0.03287)^2+(1322.55)(0.02243)^2)}}$$

$$= 1148\ rpm >> 50\ rpm$$

C-5 - Key Length

A set of calculations for gear 1 are shown below to demonstrate how the calculations of the minimum key length were done.

Knowns for Gear 1:

$$T_1 = 3151.25\ lb \cdot in \qquad d = 1.25\ in \qquad S_y = 54.3\ ksi$$

$$T_{max} = \frac{\pi d^3}{16}(0.58S_y) = \frac{\pi(1.25)^3}{16}(0.58(54300)) = 12077.80 > T_1\ acceptable$$

Minimum Length needed to Avoid Failure by Compressive Forces at Torque experienced:

$$T_1 = S_y\frac{Ld}{8}\frac{d}{2} = S_y\frac{Ld^2}{16}$$

$$3151.25 = 54300\frac{L(1.25)^2}{16}$$

$$L = 0.594\ in$$

Minimum Length needed to Avoid Failure by Key Shear at Torque experienced:

$$T_1 = 0.58S_y\frac{Ld^2}{8}$$

$$3151.25 = 0.58(54300)\frac{L(1.25)^2}{8}$$

$$L = 0.512\ in$$

Minimum length therefore is 0.594 inches.